Journal of
Medicinal Chemistry

Article

Design, Synthesis and Structure-Activity Relationships of 1,2,3-Triazole Benzenesulfonamides as new Selective Leucine-Zipper and Sterile-# Motif Kinase (ZAK) Inhibitors

Jianzhang Yang, Marthandam Asokan Shibu, Lulu Kong, Jinfeng Luo, Farheen BadrealamKhan, Yanhui Huang, Zheng-Chao Tu, Cai-Hong Yun, Chih-Yang Huang, Ke Ding, and Xiaoyun Lu

J. Med. Chem., **Just Accepted Manuscript** • DOI: 10.1021/acs.jmedchem.9b00664 • Publication Date (Web): 04 Jun 2019

Just Accepted

is published by the American Chemical Society. 1155 Sixteenth Street N.W., Washington, DC 20036

Design, Synthesis and Structure-Activity Relationships of 1,2,3-Triazole Benzenesulfonamides as new Selective Leucine-Zipper and Sterile-α Motif Kinase (ZAK) Inhibitors

Jianzhang Yang,[†#] Marthandam Asokan Shibu,[‡#] Lulu Kong,[§#] Jinfeng Luo,[‖] Farheen BadrealamKhan,[‡] Yanhui Huang,[‖] Zheng-Chao Tu,[‖] Cai-Hong Yun,[§] Chih-Yang Huang,[‡,⊥,ξ*] Ke Ding,[†*] Xiaoyun Lu[†*]*

[†]International Cooperative Laboratory of Traditional Chinese Medicine Modernization and Innovative Drug Development of Chinese Ministry of Education (MOE), College of Pharmacy, Jinan University, 601 Huangpu Avenue West, Guangzhou 510632, China

[‡]Graduate Institute of Biomedical Sciences, China Medical University, Taichung 404, Taiwan

[§]Department of Biochemistry and Biophysics, Institute of Systems Biomedicine and Beijing Key Laboratory of Tumor Systems Biology, School of Basic Medical Sciences, Peking University Health Science Center, Beijing 100191, China

[‖]Guangzhou Institutes of Biomedicine and Health, Chinese Academy of Sciences, 190 Kaiyuan Avenue, Guangzhou 510530, China

[⊥]Department of Health and Nutrition Biotechnology, Asia University, Taichung 41354, Taiwan

[ξ]College of Medicine, Hualien Tzu Chi Hospital, Buddhist Tzu Chi Medical Foundation, Tzu Chi University, Hualien 970, Taiwan

KEYWORDS: 1,2,3-triazole benzenesulfonamides, bioisoteric, ZAK, hypertrophic cardiomyopathy

ABSTRACT: ZAK is a new promising target for discovery of drugs with activity against anti-hypertrophic cardiomyopathy (HCM). A series of 1,2,3-triazole benzenesulfonamides were designed and synthesized as selective ZAK inhibitors. One of these compounds, **6p** binds tightly to ZAK protein (K_d = 8.0 nM), and potently suppresses the kinase function of ZAK with single digit nM (IC_{50} = 4.0 nM), and exhibits excellent selectivity in a KINOMEscan screening platform against a panel of 403 wild-type kinases. This compound dose-dependently blocks p38/GATA-4 and JNK/c-Jun signaling and demonstrates promising *in vivo* anti-HCM efficacy upon oral administration in a spontaneous hypertensive rat (SHR) model. Compound **6p** may serve as a lead compound for new anti-HCM drug discovery.

INTRODUCTION

Hypertrophic cardiomyopathy (HCM) is one of the most common inherited cardiovascular disorders affecting 0.2% global populations. HCM has been implied as one of the key factors causing sudden cardiac death and end-stage heart failure and stroke etc.[1,2] Typical characteristics of HCM include left ventricular hypertrophy (LVH) at a pathological level, myocyte disarray on cellular level and overexpression of brain natriuretic peptide (BNP), atrial natriuretic peptide (ANP), and β-myosin heavy chain (MHC) on molecular level.[3,4] Although a variety of genes have been reported to be involved in HCM symptoms, the molecular phenotype pathways remain unclear and the best available therapy for HCM is inadequate.[5,6] Current drug treatments for HCM include primary β-receptor blockers and calcium-channel antagonists. However, the effects of these drugs are unable to control the cardiac disorders and there is no cure for HCM.[7]

The leucine-zipper and sterile-α motif kinase (ZAK) is a member of mixed-lineage kinase (MLK) family, and widely expresses in heart, skeletal muscle, lung and pancreas.[8] Collective evidence suggested that dysregulation of ZAK is heavily involved in the development of myocardial disease, e.g. cardiac hypertrophy and myocardial fibrosis.[9-10] For instance, in H9c2 cardio myoblast cells, overexpression of ZAK leads to induction of characteristic hypertrophic features, including an increase in cell size, expression of ANF and BNP, and actin fiber organization.[10-12] ZAK-dominant negative (DN) cardiomyoblast cells are obviously resistant to hypertrophic feature transition induced by doxycycline, and the expression of ANF and BNP is also significantly down-regulated in ZAK-DN cells.[11,12] These results collectively suggest that that ZAK might be a novel promising target for anti-HCM drug discovery.[9] Recently, we reported the first "proof of concept" study that pharmacological inhibition of ZAK by a small molecule inhibitor demonstrated a therapeutic impact on cardiac hypertrophy in a SHR model.[17]

Several kinase inhibitors, such as vemurafenib (**1**, *N*-(3-(5-(4-chlorophenyl)-1*H*-pyrrolo[2,3-*b*]pyridine-3-carbonyl)-2,4-difluorophenyl)propane-1-sulfonami- de),[13] PLX-4720 (**2**, *N*-[3-[(5-chloro-1*H*-pyrrolo[2,3-*b*]pyridine-3-yl)carbonyl]-2,4-difluoro-phenyl]-1-propanesulfonamide),[13] sorafenib (**3**, 4-[4-[[[[4-chloro-3-(trifluoromethyl)phenyl]-amino]carbonyl]amino]phenoxy]-*N*-methyl-2-pyridinecarboxamide)[14] and nilotinib (4-methyl-*N*-(3-(4-methyl-1*H*-imidazol-1-yl)-5-(trifluoromethyl)-phenyl)-3-((4-(pyridin-3-yl)pyrimidin-2-yl)amino)benzamide),[15] have been reported to bind and suppress the function of ZAK. However, none of them was discovered with ZAK as the primary target.[16] Recently, a series of *N*-(3-((1*H*-pyrazolo[3,4-*b*]pyridin-5-yl)ethynyl)benzenesulfonamides were designed and synthesized by our group as a first class of selective ZAK inhibitors demonstrating promising anti-HCM therapeutic efficacy.[17] In this paper,

we report our continuous research into the design and synthesis of 1,2,3-triazole benzenesulfonamides as new selective ZAK inhibitors with *in vivo* efficacy.

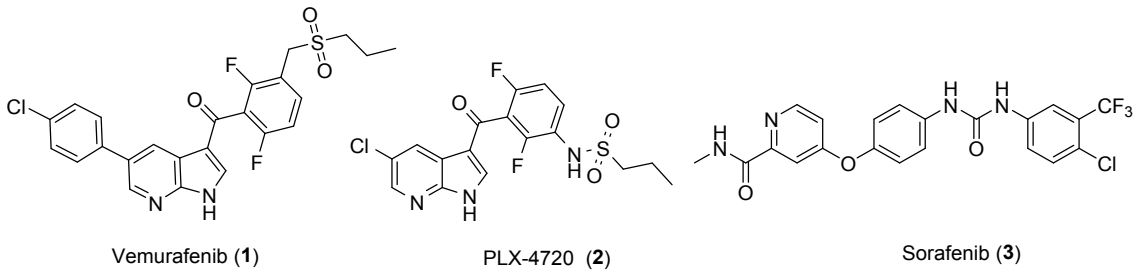

Figure 1. Reported non-selective ZAK inhibitors.

CHEMISTRY

Syntheses of the designed molecules are described in Schemes 1-4. Briefly, the commercially available difluorophenyl compound (**7**) was nitrated and coupled with the carboxylic acid (**9**) to yield the key intermediate (**10**). Reduction of **10** with Fe/HCl, followed by sulfonylation led to intermediate **11**. Cyclization of **11** with ammonium acetate, followed by deprotection with TFA produced the 1,3-imidazole **5a** (Scheme 1).

Scheme 1. Synthesis of a 1,3-imidazole **5a**

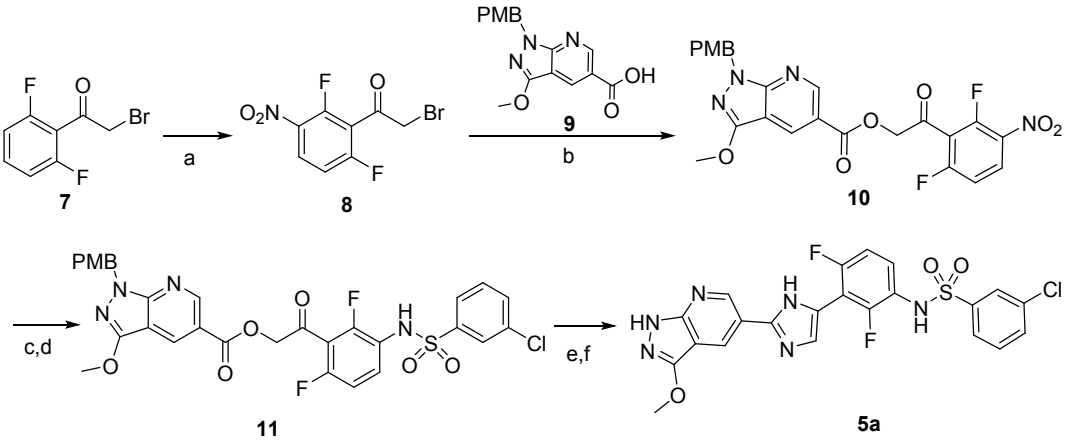

Reagents and conditions: (a) conc. HNO_3, conc. H_2SO_4, rt, 2 h, 90%; (b) (i) Cs_2CO_3, dry EtOH, 2 h; (ii) DMF, overnight 52%; (c) Fe powder, conc. HCl (aq), EtOH, H_2O, 70 °C, 2 h, 91%; (d) *m*-chlorobenzenesulfonyl chloride, pyridine, dry DCM, rt, overnight, 79%; (e) ammonium acetate, xylene, 160 °C, reflux, 82%; (f) TFA, reflux overnight, 90%.

Synthesis of a 1,3,4-oxadiazole compound (**5b**) is outlined in Scheme 2. The difluoro compound (**12**) was sulfonylated and hydrolyzed, then condensed with an acylhydrazine (**14**) to give the key intermediate **15**. Cyclization of **15** with CCl_4, Ph_3P and Et_3N, followed by deprotection with TFA led to the 1,3,4-oxadiazole (**5b**).

Scheme 2. Synthesis of a1,3,4-oxadiazole compound **5b**

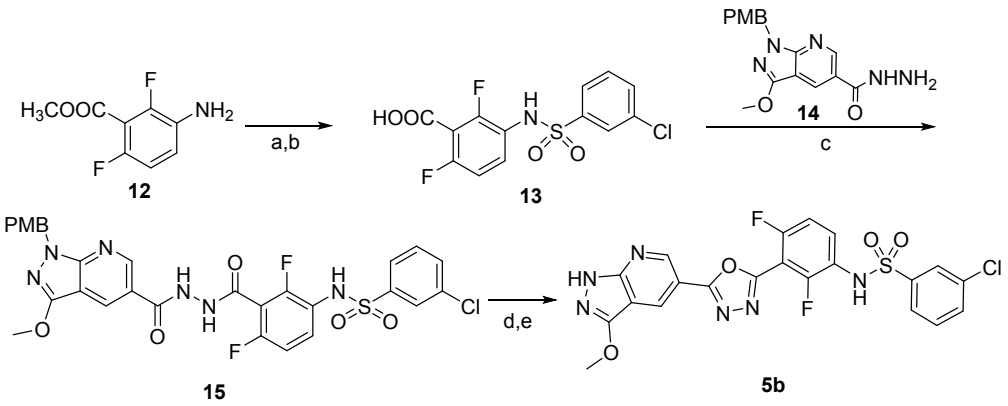

Reagents and conditions: (a) *m*-chlorobenzenesulfonyl chloride, pyridine, dry DCM, rt, overnight, 84%; (b) NaOH, EtOH, rt, 3 h, 61%; (c) HATU, DIEA, DCM, rt, 4 h, 92%; (d) Ph_3P, CCl_4, Et_3N, DMF, rt, overnight, 59%; (e) TFA, reflux, overnight, 61%.

Synthesis of the 1,2,4-oxadiazole compound (**5c**) is described in Scheme 3. Sulfonylation of the starting material (**16**) gave intermediate **17**, which reacted with hydroxylamine hydrochloride to produce (*Z*)-hydroxylcarboximidamide (**18**) in 96% yield. Condensation of **18** with **9** produced the

intermediate **19**, which was cyclized with tetrabutylammonium fluoride and deprotected to produce the 1,2,4-oxadiazole **5c**.

Scheme 3. Synthesis of a 1, 2, 4-oxadiazole compound **5c**

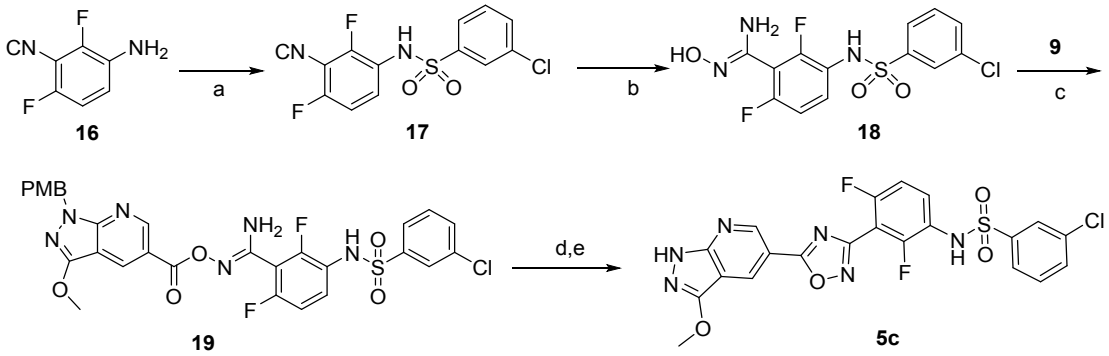

Reagents and conditions: (a) *m*-chlorobenzenesulfonyl chloride, pyridine, dry DCM, rt, overnight, 71%; (b) hydroxylamine hydrochloride, $NaHCO_3$, EtOH, reflux, 3 h, 96%; (c) HATU, DIEA, DCM, rt, 4 h, 60%; (d) tetrabutylammonium fluoride, toluene, 110 °C, reflux, 1.5 h, 82%; (e) TFA, reflux, overnight, 82%.

The 1,2,3-triazole derivatives were synthesized by following a protocol outlined in Scheme 4. Compounds **20a-20e** were diazotized with sodium nitrite to form diazonium salts, which were subsequently converted into azides (**21a-21e**). A copper-catalyzed click reaction between alkynes (**22a-22c**) and azides (**20a-20e**) generated the triazoles (**23a-23e**), which are key intermediates. Sulfonylation of **23a-23e** with substituted benzenesulfonyl chlorides followed by deprotection with TFA led to good yields of the desired compounds **5b**, **6a-6f** and **6h-6v**. Amidation of **23a** with acyl chlorides (**24a** and **24b**) followed by deprotection provided compounds **6g** and **6h**. In addition, coupling of **23a** with 1-chloro-3-isocyanobenzene (**25**), followed by deprotection gave compound **6i**.

Scheme 4. Synthesis of compounds **5d**, **6a-6f** and **6h-6v**.

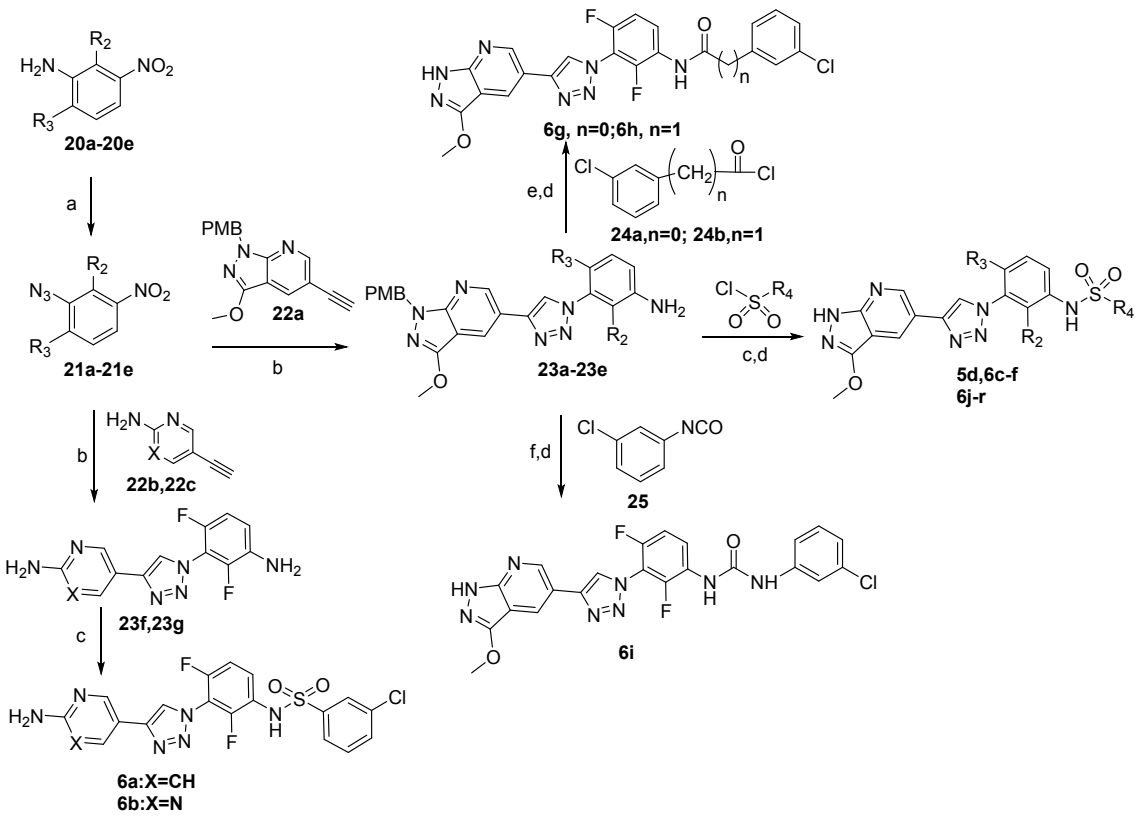

Reagents and conditions: (a) (i) TFA, 0°C, $NaNO_2$, 30 min; (ii) NaN_3, 0 °C, 2 h, 84-96%; (b) (i) sodium ascorbate, $CuSO_4 \cdot 5H_2O$, *tert*-BuOH, H_2O, 95 °C, reflux, 3 h; (ii) Fe, conc. HCl (aq), 70 °C, 2 h, 50-62% (two steps); (c) benzenesulfonyl chloride, DCM, pyridine, rt, overnight, 42%-97%; (d) TFA, reflux, overnight, 55-86%; (e) Et_3N, dry THF, 64%; (f) rt, THF, 82%.

RESULTS AND DISCUSSION

We previously reported the *N*-(3-((1*H*-pyrazolo[3,4-*b*]pyridin-5-yl)ethynyl) benzenesulfonamides (e.g. compound **4**, Figure 2) as selective ZAK inhibitors, which exhibited strong inhibitory activity against ZAK and displayed extraordinary target specificity in a KINOMEscan screening.[17] X-ray crystallographic determination revealed that the *N*-(3-((1*H*-

pyrazolo[3,4-*b*]pyridine-5-yl)ethynyl) benzenesulfonamide scaffold fits well into the active pocket of ZAK, and the alkynyl moiety served as a linking group for the pyrazolo[3,4-*b*]pyridine and the difluorobenzene (Figure 2). In our continuous efforts to identify new selective ZAK inhibitors, isosteric replacement of the alkynyl moiety with a conformationally restricted and metabolically stable heterocyclic substituent was first explored (Figure 2). The kinase inhibitory activity against ZAK was determined using a previously described protocol.[17] Inhibitory activity against B-Raf^{V600E} of these compounds was also assessed to monitor their target selectivity, because of the high sequence identity between ZAK and B-Raf^{V600E} kinase. [17]

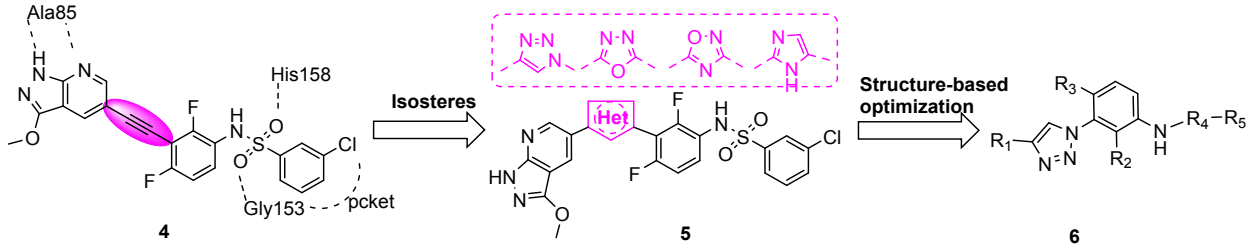

Figure 2. Optimization of 1,2,3-triazole benzenesulfonamides based on the lead compound (**4**).

The results showed that heterocyclic linkers had different impact on the ZAK inhibitory potency. For example, the 1,3,4-oxadiazole substituted analogue **5b** and the 1, 2, 4-oxadiazole substituted compound **5c** were 4.0-fold and 2.0-fold less potent than the original compound **4**, respectively, while the introduction of 1,3-imidazole linker (**5a)** caused a 66.9-fold potency loss (Table 1). Encouragingly, the 1,2,3-triazole derivative **5d** exhibited a greatly improved ZAK inhibitory activity with an IC_{50} of 1.9 nM. However, this compound also displayed relatively strong inhibition against B-Raf (IC_{50} = 198 nM). Preliminary computational investigation suggested that **5d** bound to the ATP pocket of ZAK and B-Raf^{V600E} in a similar mode to that of compound **4** (Figure 3). The 1*H*-pyrazolo[3,4-*b*]pyridine moiety could form two hydrogen bonds (HBs) with Ala85 and catch a π–π interaction with Tyr84, while the 1,2,3-triazole group had no direct

interaction with the protein, but functioned as a linking group. Two additional HBs were also made between sulfonamide group and residues His158 and Gly153. The *m*-chlorophenyl was directed towards a hydrophobic pocket formed by Leu57, Phe68 and Phe157, which was significantly different from the binding mode of **5d** with B-Raf^{V600E} where an steric hindrance with Leu505 was observed. Using **5d** as a new starting point, further medicinal chemistry optimization was conducted with the aim of improving the inhibitory potency and target specificity.

Table 1. The *in vitro* inhibitory activities of compounds **5a-5d** against ZAK and B-Raf^{V600E}.

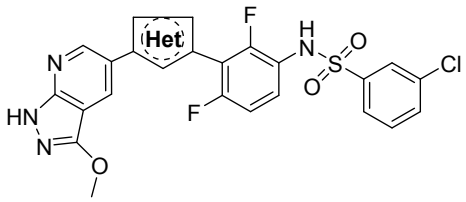

Cpds	Het	Kinase inhibition (IC_{50} nM)	
		ZAK [a]	B-Raf^{V600E} [b]
4	-	14.7 ± 3.8	>1000
5a	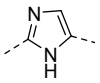	983 ± 235	>1000
5b	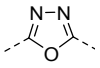	63.3 ± 20.1	>1000
5c		29.0 ± 3.7	>1000
5d		1.9 ± 0.1	198 ± 24.3

ZAK and B-Raf ^{V600E} inhibition was performed using an ADP-Glo^{TM} [a] and FRET-based Z'-Lyte kinase assay [b], repectively. The data are means from three independent experiments.

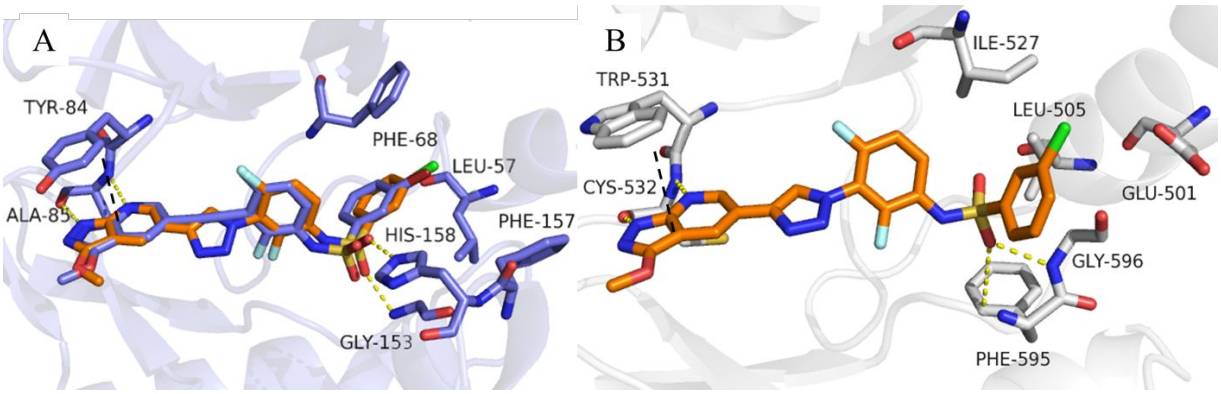

Figure 3. Computationally docking studies of **5d** with ZAK (PDB: 5X5O) (A) and B-Raf^{V600E} (PDB: 3OG7) (B). The key residues of ZAK kinase are shown in a blue and gray stick representation. Compound **5d** is shown in a blue and orange stick structure. HBs to key amino acids are indicated by yellow dashed lines.

Further computational investigation suggested that π–π stacking interactions with Tyr84 and Trp531 were critical for the 1*H*-pyrazolo[3,4-*b*]pyridine scaffold of **5d** to adopt a suitable orientation to form HBs with the hinge residues of ZAK protein (Figure 3). Substitution of the 1*H*-pyrazolo[3,4-*b*]pyridine moiety (**5d**) with a 2-pyridinyl (**6a**) and a 2-pyrimidinyl (**6b**) group indeed caused a 24-fold and 4-fold potency decrease against ZAK, respectively, while totally abolished the B-Raf^{V600E} inhibition (Table 2). Contribution of the difluoro substitution in **5d** to ZAK inhibition was also evaluated. Removal of the di-fluoro substituents resulted a 13-fold potency loss (**6c**), but the monofluoro-substituted compounds **6d** and **6e** retained strong ZAK inhibition (IC_{50} = 5.7 and 3.0 nM). However, the dichloroderivative **6f** exhibited a significantly decreased potency with an IC_{50} of 413.3 nM.

Modification of the sulfonamide part (R_4) was also conducted (Table 2) and it was shown that sulfonamide moiety in **5d** was crucial for the compound to demonstrate strong ZAK inhibition. Replacement of the sulfonamide group with an amide (**6g**), methylene amide (**6h**) or urea group

(**6i**) significantly decreased the ZAK inhibitory potency. Compound **6g**, **6h** and **6i** exhibited IC_{50} values of 54.3, 85.7 and 53 nM, respectively (Table 2).

Table 2. The *in vitro* inhibitory activities of compounds **6a-6i** against ZAK and B-Raf^{V600E}.

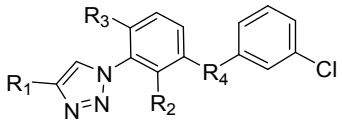

Cpds	R_1	R_2	R_3	R_4	Kinase inhibition (IC_{50} nM)	
					ZAK[a]	B-Raf^{V600E} [b]
5d	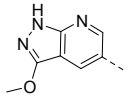	F	F		1.9±0.1	198±24.3
6a	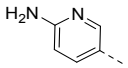	F	F		46.2±9.9	>1000
6b	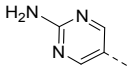	F	F		8.9±2.3	>1000
6c	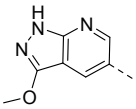	H	H		24.7±0.5	>1000
6d	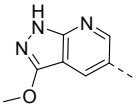	H	F		5.7±0.9	334±141nM
6e	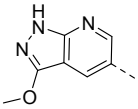	F	H		3.0±0.5	795±8.5
6f	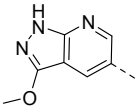	Cl	Cl		413.3±75.8	436±91.4
6g	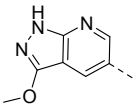	F	F		54.3±8.7	11.4±2.3
6h	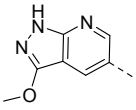	F	F		85.7±25.1	83.1±31.3

6i	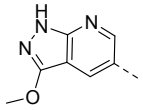	F	F	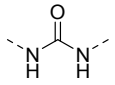	53.0±7.0	51.6±2.8

ZAK and B-Raf ^{V600E} inhibition was performed using an ADP-Glo™ [a] and FRET-based Z'-Lyte kinase assay [b], repectively. The data are means from three independent experiments.

Our previous investigation revealed that ZAK possesses a larger binding pocket comparing with that of B-Raf^{V600E} due to the outwardly shifting αC-helix.[17] It was thus hypothesized that introduction of a hydrophobic substituent to the tail phenyl group might improve the inhibitory activity and selectivity of ZAK.[17] Accordingly, extensive modification on R_5 position was conducted. The results showed that removal of the chlorine substituent (**6j**) indeed caused a 2-fold potency loss with respect to ZAK, while its inhibitory potency against B-Raf^{V600E} was obviously improved (IC_{50} = 39 nM), which was consistent to our prediction. The investigation also demonstrated that the *m*-chloro substituent could be replaced by a variety of groups such as bromo (**6k**), cyano (**6l**), methoxyl (**6m**) and methyl (**6n**) without affecting the ZAK inhibitory potency. Inhibitors **6k**, **6l**, **6m** and **6n** exhibited IC_{50} values of 2.1, 3.3, 2.4 and 4.4 nM, respectively (Table 3).

Co-crystal structure of **6k** with ZAK determination validated our proposed binding mode of the molecules (Figure 4). Consistent to our prediction, the 1*H*-pyrazolo[3,4-*b*]pyridine moiety made two HBs with Ala85, and captured an additional HB and a π−π interaction with Tyr84. The 1,2,3-triazole forms a HB network with Lys45 and Asp151 mediated by H_2O. The sulfonamide participated in a single HB interaction with Gly153 because of the rotation of His158. Similar to our previous observation,[17] the *m*-bromophenyl moiety could induce an obviously outward extension of αC helix and caused a rotation of Leu57 to avoid steric hindrance with **6k** (Figure 4).

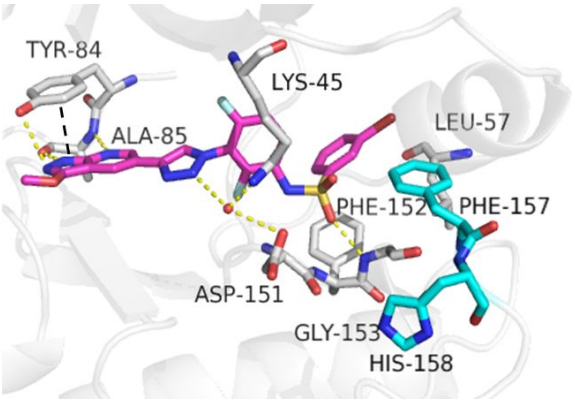

Figure 4. Co-crystal structure of ZAK and **6k** (PDB: 6JUT). Compound **6k** is shown in purple stick structure. The key residues of ZAK kinase are shown in gray and cyan sticks. Hydrogen bonds to key amino acids are indicated by yellow dashed lines.

Based on the structural information, it was further hypothesized that a large hydrophobic group might be accommodated at the R_5 position to achieve strong and selective ZAK inhibition. Indeed, *m*-isopropyl phenyl (**6o**), *m*-biphenyl (**6p**), 2-naphthyl (**6q**) and 1-naphthyl (**6r**) analogues retained strong ZAK inhibitory activities with IC_{50} values of 6.9, 4.0, 4.5 and 4.2 nM, respectively. Significatly, the *m*-biphenyl-substituted molecule (**6p**) totally abolished the inhibition against B-Raf^{V600E}, becoming one of the most potent and selective ZAK inhibitors in this series.

Table 3. *In vitro* inhibitory activities of compounds **6j-6r** against ZAK and B-Raf ^{V600E}.

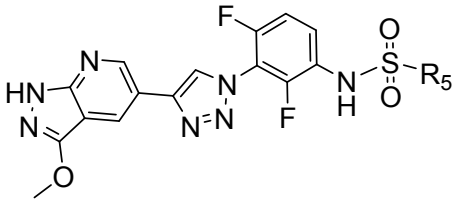

Cpds	R_5	Kinase inhibition (IC_{50} nM)	
		ZAK[a]	B-Raf^{V600E} [b]

5d	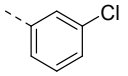	1.9±0.1	198±24.3
6j		3.8±1.8	39±11.6
6k	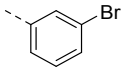	2.1±0.3	272.3±68.9
6l	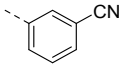	3.3±0.5	470.3±165.6
6m	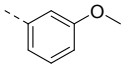	2.3±0.4	272±35.8
6n	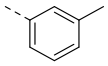	4.4±1.1	453±98
6o	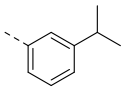	6.9±1.2	190±73.9
6p	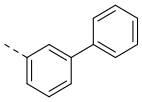	4.0±1.0	>1000
6q	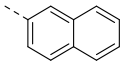	4.5±0.6	856±75.2
6r	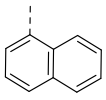	4.2±1.4	125.7±18.3

ZAK and B-Raf ^{V600E} inhibition was performed using an ADP-Glo™ [a] and FRET-based Z'-Lyte kinase assay [b], repectively. The data are means from three independent experiments.

The ZAK inhibition by **6p** was validated by determining its binding affinity with an active site-dependent competition binding assay (DiscoveRx, San Diego, CA).[18] Compound **6p** bound tightly to the ATP-binding site of ZAK (K_d = 8.0 nM), validating its strong kinase inhibition against ZAK. The target selectivity of **6p** was also evaluated by using a KINOMEscan study against 468 kinases at 1.0 μM (Figure 5A). The results revealed that **6p** displayed an excellent target selectivity profile (see Supporting information, Table S1).[18] Several kinases, e.g. abelson

murine leukemia viral oncogene homolog 1 (ABL1), B lymphoid tyrosine kinase (BLK), FMS-like tyrosine kinase 3 (FLT3 ITD, F691L), lymphocyte-specific protein tyrosine kinase (LCK), LIM domain kinase 1 (LIMK1), LIM domain kinase 2 (LIMK2) and receptor-interacting serine/threonine-protein kinase 2 (RIPK2) were identified as the major "off targets" (inhibition > 90%, ctrl% < 10) (Figure 5B). Further evaluation reveled that **6p** demonstrated 2-66- fold target selectivity over these "off targets" (Figure 5B). Kinase activity determination also showed that **6p** inhibited ABL1 with an IC_{50} of 156 nM, which was approximate 30 folds less potent than that of ZAK kinase (Figure 5B).

A

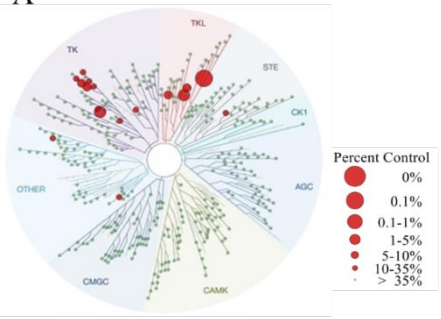

B

Kinase	K_d value (nM)
ZAK	8
ABL1	15
BLK	190
FLT3(ITD, F691L)	530
LCK	160
LIMK1	23
LIMK2	63
RIPK2	57

Figure 5. KINOMEscan profiling of **6p**. (A) KINOMEscan profiling of **6p** at a concentration of 1.0 μM against 468 kinases. (B) The K_d determination of compound **6p** against the potential off targets.

Collective studies have suggested that activation of ZAKα signaling is critical for cardiac hypertrophy.[19,20] The inhibitory effects of **6p** on the activation of ZAKα were therefore investigated in H9c2 cells (Figure 6A). The results showed that **6p** dose-dependently inhibited the phosphorylated ZAKα, but had no detectable impact on the ZAKα expression level. Consequently, an *in vitro* AngII induced H9c2 cardio myoblast cell model was utilized to evaluate the therapeutic effect of **6p** on hypertrophy. The results showed that AngII obviously elevated the expression of

BNP and ZAKα downstream MAPK kinases, e.g. p38 and JNK. Whereas, compound **6p** potently suppressed phosphorylation of p38, JNK and dose-dependently decreased the expression of BNP in H9c2 cardio myoblast cells. The results demonstrated the blockage of **6p** on the myocardial hypertrophy process induced by the AngII (Figure 6B).

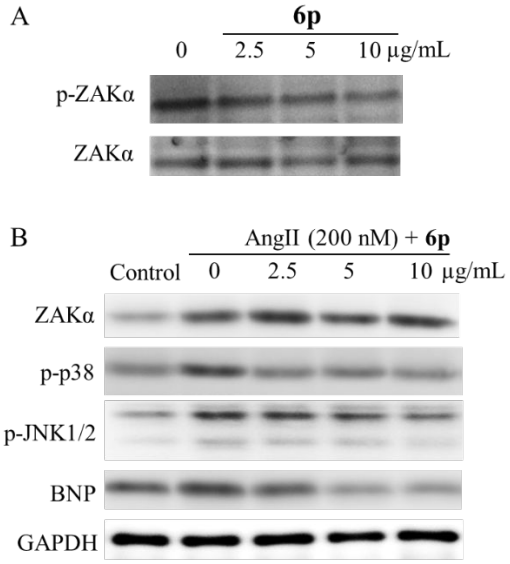

Figure 6. (A) Effects of p-ZAKα and ZAKα inhibition by **6p** in H9c2 cells. (B) Effects of ZAKα downstream signaling inhibition by **6p** in AngII induced H9c2 cells. The data means from three independent experiments

The potential therapeutic effect of **6p** was further validated in a cell-based Tet-on ZAKα system (Figures 7 and 8).[21] It was shown that doxycycline (Dox) significantly induced Z hypertrophic effects in H9c2 cells with increased cell surface area and elongation of actin filaments as determined by F-actin staining (Figures 7A and 7B), but hypertrophic phenomena could be potently suppressed by a ZAK inhibitor **6p** in a dose-dependent manner (Figure 7A and 7B). The results also showed that Dox obviously induced ZAKα expression in a Tet-on ZAKα system, leading to the elevation of p-JNK and p-p38 (Figures 8A and 8B) and hypertrophic transcription

factors p-GATA-4 and p-c-Jun (Figures 8C and 8D). Whereas, the activation of these key factors could be evidently suppressed by compound **6p** (Figures 8C and 8D). The immunofluorescence staining further showed that ZAKα overexpression obviously elevated the nuclear translocation of p-GATA-4, while the corresponding processes were potently suppressed by **6p**. These results further validated that compound **6p** could effectively suppress hypertrophy induced by ZAKα overexpression by blocking p38/GATA-4 and JNK/c-Jun signaling.[9]

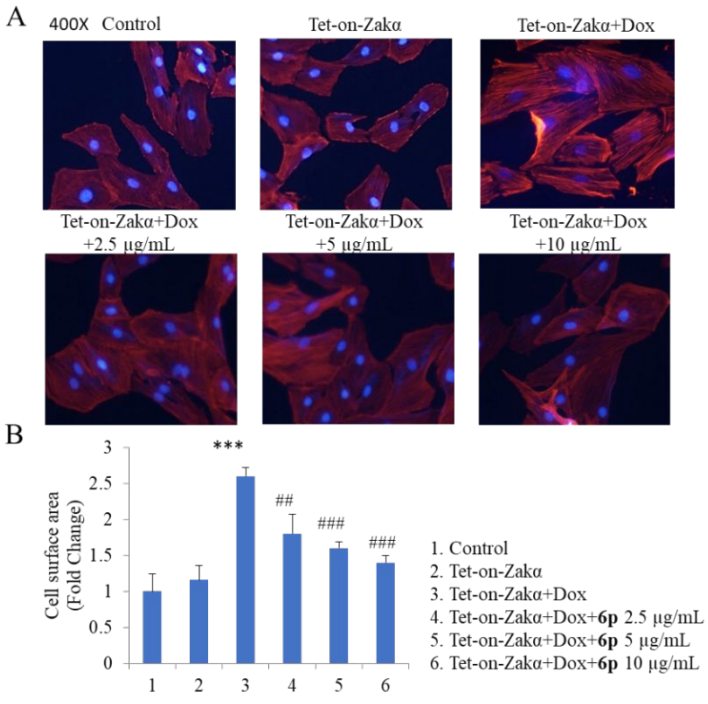

Figure 7. Effects of **6p** suppressing the hypertrophic effects of ZAKα in a Tet-on ZAKα system. A) Cells were cultured in serum-free medium for 12 h, and treated with Dox (2 μg/mL) and **6p** (2.5, 5 and 10 μg/mL) for 24 h, then stained with phalloidin-rhodamine to measure the cell size. DAPI staining was used to mark nuclei. B) The statistical results were shown from three independent experiment (***p<0.001, compared with control group ##p<0.01, ###p<0.001 compared with Dox group)

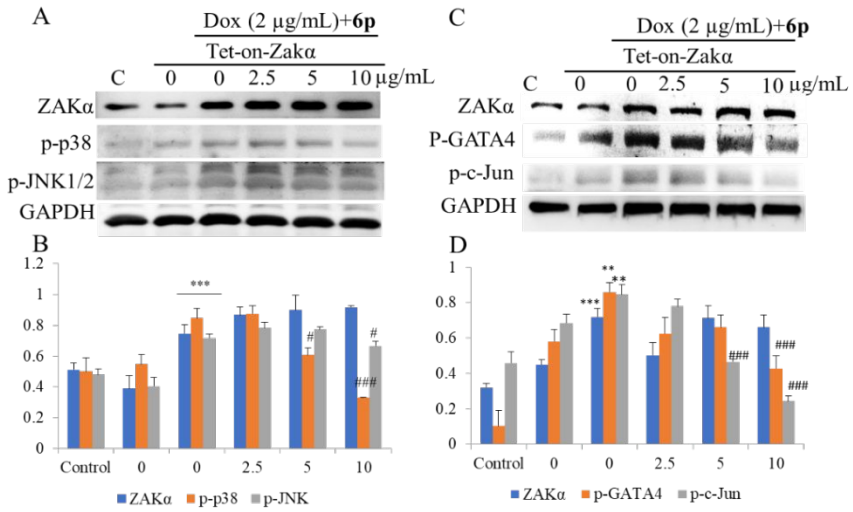

Figure 8. Effects of **6p** suppressing the p-JNK and p-p38 and downregulating the levels of p-GATA-4 (A and B) and p-c-Jun (C and D). The statistical results were shown from three independent experiment (***p*<0.01, ****p*<0.001 compared with control group; # *p*<0.05, ##*p*<0.01, ###*p*<0.001 compared with Dox group)

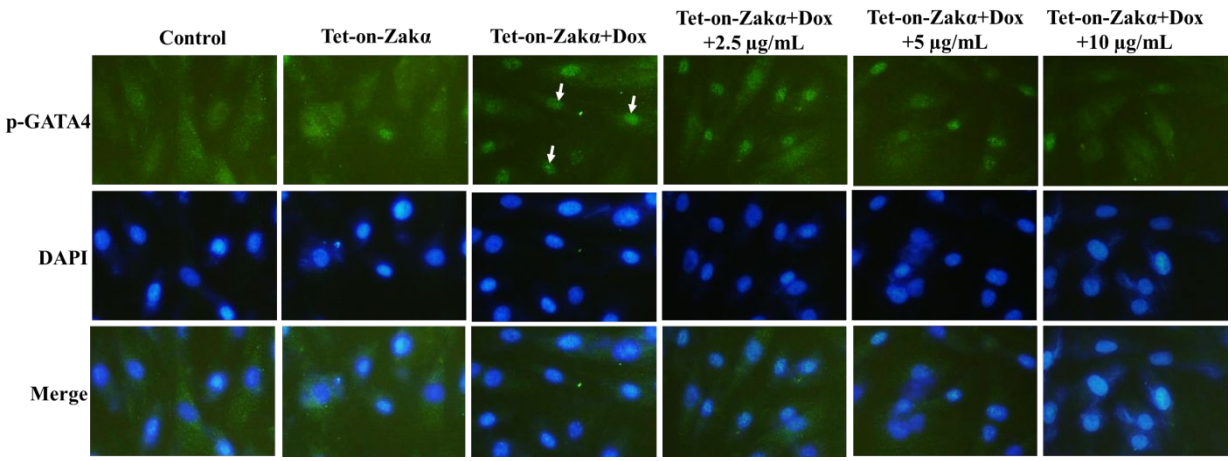

Figure 9. Immunofluorescence staining for p-GATA4. The cells were incubated at 4 ℃ overnight with primary antibody (1:400 diluted with 1% BSA in PBS), then washed with PBS and incubated in diluted secondary antibody and incubated in the dark at 37 °C for 1 h. The cells were

subsequently counterstained by 4′,6-diamidino-2-phenylindole (DAPI) nuclear stain. The arrows in the Tet-on-Zakα+Dox group indicate nuclear localisation of p-GATA-4.

The *in vivo* pharmacokinetic (PK) profiles of **6p** were also determined in Sprague-Dawley (SD) rats (Table 4). It was shown that compound **6p** displays encouraging PK profiles with an oral AUC value of 71790.9 ug/L·h, a half-life value ($T_{1/2}$) of 1.7 hr and an oral bioavailability of 65.3%. These data provided a foundation for the follow-up *in vivo* oral dosing regimen.

Table 4. Pharmacokinetic profiles of compound **6p** in rats.

parameters	po (10mg/kg)	iv (2.5 mg/kg)
AUC(0-∞) ug/L*h	71790.9	27866.1
AUC(0-t) ug/L*h	71572.6	27424.4
$T_{1/2}$ (h)	1.7	1.6
C_{max} (ug/L)	16372.2	34151.6
CL(L/h/kg)	nd	91.9
BA (%)	65.3	

nd. Not determined.

The spontaneous hypertensive rats (SHR) model was utilized to investigate the potential *in vivo* anti-HCM effects of **6p** with the normotensive Wistar-Kyoto (WKY) rat as a control. The results showed that the SHR performed greater left ventricular masses than normotensive WKY rats, indicating the symptoms of hypertrophy (Table 4). Compound **6p** was orally administrated at 0, 2.5 and 10 mg/kg once daily for 8 weeks. The whole heart (WH) and the left ventricle (LV) were collected for biological determination after the experimental rats were sacrificed. The results demonstrated that compound **6p** suppressed the WH and LV mass elevation and rescued the hypertrophic symptoms in a dose-dependent manner (Table 5). Briefly, the average LVW value was 0.89 g for the vehicle control SHRs, while the corresponding values were decreased to 0.82

and 0.78 g, respectively, after treatment with 2.5 mg/kg and 10 mg/kg of **6p.** Western blot analysis showed that the hypertrophy-related signaling mediators and markers such as p-JNK, p-c-Jun, p-GATA-4, p-P38 and ANP were considerably higher in SHR than that in the normotensive WKY control rats (Figures 10A and 10B). Consistent to the observation in cell-based models, compound **6p** suppressed the phosphorylation of ZAK downstream signaling JNK, p38, c-Jun, p-GATA-4 and protein levels of hypertrophic markers BNP and ANP in a dose-dependent manner. Hematoxylin and eosin (H&E) staining investigation also showed normal alignment of cardiomyocytes in the normotensive WKY control tissues, while much more interstitial spaces in the SHRs heart tissues (Figure 10C). Whereas, the myocardial cell disarrangement was significantly relieved by **6p** to normal phenomena (Figure 10C). The studies further supported the oral therapeutic effects of **6p** on cardiac hypertrophy in SHRs by suppression of ZAK downstream p38/GATA-4 and JNK/c-Jun signaling.

Table 5. Compound **6p** dose-dependently inhibits myocardial hypertrophy *in vivo*.

Weight (g)	**WKY**	**SHR**	**6p-2.5 mg/kg**	**6p-10 mg/kg**
Whole heart (WHW)	1.08±0.009	1.23±0.006$^{###}$	1.18±0.008	1.13±0.005**
Left ventricular (LVW)	0.70±0.007	0.89±0.005$^{###}$	0.82±0.007	0.78±0.007***

Values are Mean ± SD; Statistical significance: $^{###}$ P≤ 0.001 vs WKY; **P ≤ 0.01; ***P ≤ 0.001 vs SHR group

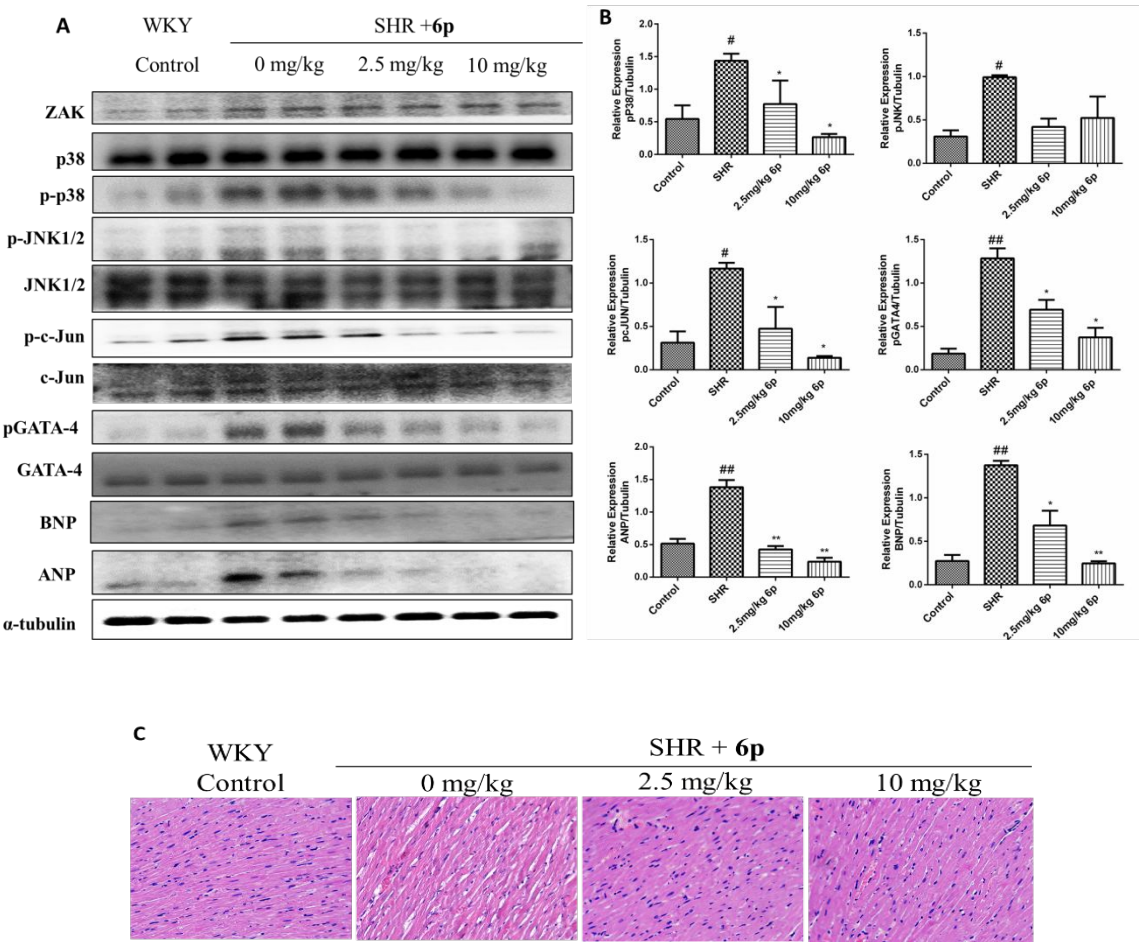

Figure 10. (A) Effects of **6p** suppressing the phosphorylation of ZAK downstream signaling of JNK, p38, c-Jun and GATA-4, and the expression of hypertrophic marker proteins (BNP and ANP) *in vivo*. (B) The statistical results from three independent experiments are shown. (C) H&E staining investigation of the heart tissues by treatment of **6p**. Statistical significance: $^{\#}P \leqslant 0.05$ and $^{\#\#}P \leqslant 0.01$ compared to WKY Control; $^{*}P \leqslant 0.05$ and $^{**}P \leqslant 0.01$ compared to SHR

CONCLUSION

A series of 1,2,3-triazole benzenesulfonamides were designed and optimized as novel selective inhibitors of ZAK. One of the most potent compounds, **6p** bound tightly to ZAK with a K_d of 8.0 nM, and potently inhibited ZAK activity with an IC_{50} of 4.0 nM, while it was significantly less

potent on majority of the evaluated kinases at 1.0 μM in KINOMEscan profiling. The compound significantly suppressed the ZAK overexpression induced hypertrophy both *in vitro* and *in vivo* by blocking p38/GATA-4 and JNK/c-Jun signaling, and displayed promising anti-HCM effect in the SHR model at the low dose (10mg/kg). Compound **6p** may be utilized as a promising lead compound for further development.

EXPERIMENTAL SECTION

General Methods for Chemistry. All commercially available reagents and solvents were used as received. All reactions were monitored by thin layer chromatography (TLC). Compounds were detected by ultraviolet light (UV) absorption at either 254 or 365 nm. Column chromatography was used with silica gel 300 mesh. ^{1}H NMR, spectra were performed with Bruker AV-400 spectrometer, ^{13}C NMR spectra were performed on Bruker AV-400 spectrometer at 101 MHz, internal reference was either TMS or deuterated NMR solvent. The low resolution mass was performed on an Agilent 1200 HPLC-MSD mass spectrometer. High resolution mass spectral analysis was performed on an Applied Biosystems Q-STAR Elite ESI-LC-MS/MS mass spectrometer. Purity of all final compounds were confirmed to be >95% by HPLC analysis with the Agilent 1260 system. The analytical columns were YMC-Triart C_{18} reversed-phase column, 5 μm, 4.6×250 mm, flow rate 1.0 mL/min.

General Procedure A for Sulfonylation:

Sulfonyl chlorides (1.2 equiv) and pyridine (1.5 equiv) were gradually added dropwise to a solution of anilines (1.0 equiv) in anhydrous DCM (20 mL), then stirred at r.t. overnight. The mixture was concentrated *in vacuo* and purified by column chromatography (25-50% EtOAc in petroleum ether) to produce the desired compounds in 42%-97% yields.

General Procedure B for PMB deprotection:

Benzenesulfonamides (0.15 mmol) were refluxed with trifluoroacetic acid (5 mL) overnight, then cooled to r.t. and concentrated *in vacuo*. The mixture was quenched with H_2O, neutralized to pH 7 with saturated $NaHCO_3$ solution and extracted with EtOAc three times. The combined organic phases were washed with brine, dried over anhydrous sodium sulfate and evaporated. The crude material was further purified by flash column chromatography eluting with 1.25-2.5% MeOH in DCM to produce the desired compounds. (Yield: 55%-86%).

3-Chloro-*N*-(2,4-difluoro-3-(5-(3-methoxy-1*H*-pyrazolo[3,4-*b*]pyridin-5-yl)-1*H*-imidazol-2-yl)phenyl)benzenesulfonamide (5a)

Compound **11** (100 mg, 0.15 mmol) and ammonium acetate (59 mg, 7.6 mmol) were dissolved in xylene (25 mL), then stirred at 160 °C overnight (TLC: EtOAc: petroleum ether = 1: 1, Rf~0.4). The mixture was concentrated in vacuo and purified by column chromatography (40% EtOAc in petroleum ether) to afford PMB protection 1,3-imidazole compound as a yellow solid (80 mg, yield 82%). ^{1}H NMR (400 MHz, DMSO-d_6) δ 12.99 (s, 1H), 10.36 (s, 1H), 9.14 (d, J = 2.0 Hz, 1H), 8.59 (d, J = 2.0 Hz, 1H), 7.76 (p, J= 3.5 Hz, 2H), 7.70-7.67 (m, 1H), 7.62 (t, J = 8.2 Hz, 1H), 7.53 (s, 1H), 7.24-7.20 (m, 2H), 7.16 (d, J = 8.8 Hz, 1H), 6.90-6.86 (m, 2H), 5.47 (s, 2H), 4.03 (d, J = 4.0 Hz, 3H), 3.71 (s, 3H).

The above product was treated according to the general procedure B to afford **5a** as a white solid. (Yield: 90%; TLC: EtOAc: petroleum ether = 1: 1, Rf~0.1). ^{1}H NMR (400 MHz, DMSO-d_6) δ 12.98 (s, 1H), 12.77 (s, 1H), 10.40 (s, 1H), 9.12 (s, 1H), 8.60 (s, 1H), 7.75 (d, J = 10.2 Hz, 2H), 7.69 (d, J = 7.8 Hz, 1H), 7.62 (t, J = 7.8 Hz, 1H), 7.52 (s, 1H), 7.27-7.07 (m, 2H), 4.05 (s, 3H). ^{13}C NMR (101 MHz, DMSO-d_6) δ 159.06, 156.53, 155.59, 152.87, 152.16, 148.30, 144.88,

142.03, 134.29, 133.48, 131.82, 129.35, 126.58, 125.77, 125.34, 121.17, 119.82, 119.05, 113.14, 112.19 (d, *J*= 25.5 Hz, 1C), 103.49, 56.25. HPLC analysis: MeOH: H_2O (50: 50), 15.32 min; purity: 97.4%. HRMS (ESI) for $C_{22}H_{15}ClF_2N_6O_3S$ $[M+H]^+$, calcd: 517.0656; found: 517.0648.

3-Chloro-*N*-(2,4-difluoro-3-(5-(3-methoxy-1*H*-pyrazolo[3,4-*b*]pyridin-5-yl)-1,3,4-oxadiazol -2-yl)phenyl)benzenesulfonamide (5b)

A mixture of compound **15** (1.4 g, 2.17 mmol), triphenyl-phosphine (682 mg, 2.6 mmol), CCl_4 (400 mg, 2.6 mmol) and DIPEA (420 mg, 3.3 mmol) in DMF (50 mL) was stirred at r.t. under argon for overnight (monitored by TLC: EtOAc: petroleum ether = 1: 1, Rf~0.7). The mixture was quenched with H_2O and extracted with EtOAc three times. The organic phases were washed with brine, dried over anhydrous Na_2SO_4 and evaporated. The residue was purified by flash column chromatography (30% EtOAc in petroleum ether) to obtain PMB protection 1,3,4-oxadiazol compound as a yellow solid (800 mg, yield 59%). ^{1}H NMR (400 MHz, DMSO-d_6) δ 10.82 (s, 1H), 9.16 (d, *J* = 2.0 Hz, 1H), 8.61 (d, *J* = 2.1 Hz, 1H), 7.82 (t, *J* = 1.9 Hz, 1H), 7.77 (dd, *J* = 8.0, 2.1 Hz, 1H), 7.73-7.69 (m, 1H), 7.63 (t, *J* = 7.9 Hz, 1H), 7.53 (d, *J* = 5.7 Hz, 1H), 7.41 (d, *J* = 9.5 Hz, 1H), 7.28-7.21 (m, 2H), 6.92-6.85 (m, 2H), 5.51 (s, 2H), 4.06 (s, 3H), 3.71 (s, 3H).

The above product was treated by the general procedure B to afford **5b** as white solid (Yield: 61%; TLC: EtOAc: petroleum ether = 1: 1, Rf~0.2). ^{1}H NMR (400 MHz, DMSO-d_6) δ 13.17 (s, 1H), 10.66 (s, 1H), 9.10 (d, *J* = 2.0 Hz, 1H), 8.59 (d, *J* = 2.0 Hz, 1H), 7.79 (dd, *J* = 7.4, 1.4 Hz, 2H), 7.70 (dt, *J* = 7.8, 1.6 Hz, 1H), 7.64 (t, *J* = 7.9 Hz, 1H), 7.57 (td, *J* = 8.9, 5.6 Hz,1H), 7.46-7.39 (m, 1H), 4.08 (s, 3H). ^{13}C NMR (101 MHz, DMSO-d_6) δ 164.10, 159.19, 156.61, 156.05, 155.97, 152.91, 148.38, 141.75, 134.42, 133.68, 132.39 (d, *J* = 10.1 Hz, 1C), 131.97, 128.50, 126.60, 125.84, 122.03 (d, *J* = 13.0 Hz, 1C), 113.72 (d, *J* = 22.3 Hz, 1C), 111.79, 103.68, 103.25

(d, *J* = 17.5 Hz, 1C), 56.43. HPLC analysis: MeOH: H_2O (50: 50), 20.21 min; purity:100%. HRMS (ESI) for $C_{21}H_{13}ClF_2N_6O_4S$ $[M+H]^+$, calcd: 519.0448; found: 519.0448.

3-Chloro-*N*-(2,4-difluoro-3-(5-(3-methoxy-1*H*-pyrazolo[3,4-*b*]pyridin-5-yl)-1,2,4-oxadiazol-3-yl)phenyl)benzenesulfonamide (5c)

Compound **19** (100 mg, 0.15 mmol) and tetra-butylammonium fluoride (1.0 M solution in THF, 0.18 mL) were added in toluene and the mixture was refluxed at 110 °C for 1.5 h monitored by TLC (EtOAc: petroleum ether = 1: 5, Rf~0.3). The mixture was concentrated in vacuo, and purified by column chromatography (20% EtOAc in petroleum ether) to obtain PMB protection 1,2,4-oxadiazol compound as a yellow solid (80 mg, yield 82%). ^{1}H NMR (400 MHz, DMSO-d_6) δ 10.61 (s, 1H), 9.23 (t, *J* = 1.8 Hz, 1H), 8.83 (t, *J* = 1.8 Hz, 1H), 7.80-7.75 (m, 2H), 7.71-7.67 (m, 1H), 7.64 (dd, *J* = 8.2, 1.6 Hz, 1H), 7.54 (d, *J* = 6.8 Hz, 1H), 7.38 (t, *J* = 8.9 Hz, 1H), 7.28-7.22 (m, 2H), 6.89 (dd, *J* = 8.6, 1.7 Hz, 2H), 5.52 (s, 2H), 4.06 (d, *J* = 1.5 Hz, 3H), 3.72 (d, *J* = 1.5 Hz, 3H).

The above product was treated by the general procedure B to afford **5c** as a white solid. (Yield: 82%; EtOAc: petroleum ether = 1: 3, TLC Rf~0.2). ^{1}H NMR (400 MHz, DMSO-d_6) δ 13.25 (s, 1H), 10.62 (s, 1H), 9.17 (d, *J* = 2.1 Hz, 1H), 8.80 (d, *J* = 2.1 Hz, 1H), 7.77 (dt, *J* = 4.1, 1.8 Hz, 2H), 7.71-7.66 (m, 1H), 7.63 (dd, *J* = 10.1, 6.2 Hz, 1H), 7.53 (td, *J* = 8.8, 5.6 Hz, 1H), 7.37 (t, *J* = 9.1 Hz, 1H), 4.08 (s, 3H). ^{13}C NMR (101 MHz, DMSO-d_6) δ 175.33, 160.80, 159.44, 156.90, 156.30, 153.17, 149.53, 141.89, 134.39, 133.64, 131.93, 131.78 (d, *J* = 11.1 Hz, 1C), 130.38, 126.54, 125.76, 121.91 (d, *J* = 14.1 Hz, 1C), 113.27 (d, *J* = 20.2 Hz, 1C), 111.94, 105.72 (t, *J* = 17.2 Hz, 1C), 103.87, 56.50. HPLC analysis: MeOH: H_2O (50: 50), 26.99 min; purity: 100%. HRMS (ESI) for $C_{21}H_{13}ClF_2N_6O_4S[M+H]^+$, calcd: 519.0448; found: 519.0443.

3-Chloro-*N*-(2,4-difluoro-3-(4-(3-methoxy-1*H*-pyrazolo[3,4-*b*]pyridin-5-yl)-1*H*-1,2,3-triazol-1-yl)phenyl)benzenesulfonamide (5d)

5d was synthesized from **23a** (120 mg, 0.26 mmol) with general procedure A to produce 4-chloro-*N*-(2,4-difluoro-3-(4-(3-methoxy-1-(4-methoxybenzyl)-1*H*-pyrazolo[3,4-*b*]-pyridinyl)-1*H*-1,2,3-triazol-1-yl)phenyl)benzenesulfo namideas a yellow solid (135 mg, yield 82%; TLC: EtOAc/petroleum ether=1:3, Rf~0.3). ^{1}H NMR (400 MHz, DMSO-d_6) δ 10.75 (s, 1H), 9.12 (d, J = 2.0 Hz, 1H), 9.11 (s, 1H), 8.58 (d, J = 2.0 Hz, 1H), 7.83-7.77 (m, 2H), 7.74-7.70 (m, 1H), 7.66 (d, J = 7.8 Hz, 1H), 7.51 (d, J = 8.5 Hz, 2H), 7.26-7.21 (m, 2H), 6.90-6.86 (m, 2H), 5.48 (s, 2H), 4.04 (s, 3H), 3.71 (s, 3H). HRMS (ESI) for $C_{29}H_{22}ClF_2N_7O_4S$ $[M+H]^+$, calcd: 638.1183; found: 638.1184.

The above product was treated by the general procedure B to afford **5d** as a white solid. (Yield: 76%; TLC: EtOAc: petroleum ether = 1:3, Rf~0.1). ^{1}H NMR (400 MHz, DMSO-d_6) δ 12.76 (s, 1H), 10.75 (s, 1H), 9.09 (s, 1H), 9.06 (d, J = 2.0 Hz, 1H), 8.56 (d, J = 2.0 Hz, 1H), 7.82-7.76 (m, 2H), 7.72 (d, J = 7.9 Hz, 1H), 7.65 (t, J = 7.8 Hz, 1H), 7.56-7.46 (m, 2H), 4.05 (s, 3H). ^{13}C NMR (101 MHz, DMSO-d_6) δ 155.44, 152.91, 152.44, 149.97, 148.18, 145.32, 142.17, 134.41, 133.63, 131.96, 129.62 (d, J = 8.4 Hz, 1C), 126.58, 125.84, 125.76, 124.38, 122.79 (d, J = 11.1 Hz, 1C), 118.41, 115.45 (t, J = 14.8 Hz, 1C), 113.11 (d, J = 20.4 Hz, 1C), 103.79, 56.17. HPLC analysis: MeOH: H_2O (50: 50), 9.61 min, 97.8% purity. HRMS (ESI) for $C_{21}H_{14}ClF_2N_7O_3S$ $[M+H]^+$, calcd: 518.0608; found: 518.0601.

***N*-(3-(4-(6-Aminopyridin-3-yl)-1*H*-1,2,3-triazol-1-yl)-2,4-difluorophenyl)-3-chloro-benzenesulfonamide (6a)**

Compound **6a** was synthesized from **23f** (60 mg, 0.21 mmol) with the general procedure A as a white solid (44 mg, yield 50%; TLC: EtOAc: petroleum ether = 1: 1, Rf~0.5). ^{1}H NMR (400 MHz, DMSO-d_6) δ 10.79 (s, 1H), 8.80 (s, 1H), 8.49-8.40 (m, 1H), 7.87 (dd, J = 8.6, 2.4 Hz, 1H), 7.78 (d, J = 8.6 Hz, 2H), 7.71 (d, J = 7.8 Hz, 1H), 7.64 (t, J = 7.8 Hz, 1H), 7.53-7.42 (m, 2H), 6.56 (d, J = 8.6 Hz, 1H), 6.29 (s, 2H). ^{13}C NMR (101 MHz, DMSO-d_6) δ 160.19, 154.85, 152.36, 149.82, 145.64 (d, J = 8.3 Hz, 1C), 142.84, 134.93, 134.29, 133.25, 131.83, 128.73, (d, J = 9.1 Hz, 1C), 126.54, 125.70, 124.12 (d, J = 11.1Hz, 1C), 122.67, 115.51 (t, J = 14.1 Hz, 1C), 114.47, 112.85 (d, J = 20.2 Hz, 1C), 108.51. HPLC analysis: MeOH: H_2O (55: 45), 3.65 min, 97.6% purity. HRMS (ESI) for chemical formula: $C_{19}H_{13}ClF_2N_6O_2S[M+H]^+$, calcd: 463.0550; found: 463.0540.

***N*-(3-(4-(2-Aminopyrimidin-5-yl)-1*H*-1,2,3-triazol-1-yl)-2,4-difluorophenyl)-3-chloro-benzenesulfonamide (6b)**

Compound **6b** was synthesized from **23g** (70 mg, 0.24 mmol) with the general procedure A as a white solid (69 mg, yield 62%; TLC: MeOH: DCM = 1: 15, Rf~0.5). ^{1}H NMR (400 MHz, DMSO-d_6) δ 10.75 (s, 1H), 8.89 (s, 1H), 8.75 (s, 2H), 7.79 (dd, J = 7.9, 1.4 Hz, 2H), 7.71 (dt, J = 7.9, 1.5 Hz, 1H), 7.65 (t, J = 7.8 Hz, 1H), 7.55-7.44 (m, 2H), 7.03 (s, 2H). ^{13}C NMR (101 MHz, DMSO-d_6) δ 163.58, 155.78 (s, 2C), 153.20, 152.60, 150.04, 143.21, 141.74, 134.45, 133.81, 132.02, 129.97 (d, J = 9.4 Hz, 1C), 126.59, 125.80, 123.16, 122.16 (d, J = 11.7 Hz, 1C), 115.47 (t, J = 14.7 Hz, 1C), 113.18 (t, J = 10.5 Hz, 1C). HPLC analysis: MeOH: H_2O (50: 50), 8.36 min; purity: 100%. HRMS (ESI) for chemical formula: $C_{18}H_{12}ClF_2N_7O_2S$ $[M+H]^+$, calcd: 464.0503; found: 464.0505.

3-Chloro-*N*-(3-(4-(3-methoxy-1*H*-pyrazolo[3,4-*b*]pyridin-5-yl)-1*H*-1,2,3-triazol-1-yl)-phenyl)benzenesulfonamide(6c)

Compound **6c** was synthesized from **23b** by a procedure similar to that of **5d** (Yield: 59% (two steps); TLC: EtOAc: petroleum ether = 1: 2, Rf~0.2). ^{1}H NMR (400 MHz, DMSO-d_6) δ 12.75 (s, 1H), 10.86 (s, 1H), 9.36 (s, 1H), 9.09 (d, J = 2.0 Hz, 1H), 8.58 (d, J = 2.0 Hz, 1H), 7.86 (t, J = 1.9 Hz, 1H), 7.79 (ddt, J = 3.8, 2.7, 1.3 Hz, 2H), 7.74 (ddd, J = 8.1, 2.2, 1.1 Hz, 1H), 7.65-7.58 (m, 2H), 7.54 (t, J = 8.0 Hz, 1H), 4.06 (s, 3H). ^{13}C NMR (101 MHz, DMSO-d_6) δ 155.43, 152.38, 148.11, 145.95, 141.39, 139.25, 137.61, 134.46, 133.74, 132.01, 131.53, 126.72, 125.92, 125.65, 120.33, 119.86, 118.84, 116.06, 111.70, 103.80, 56.18. HPLC analysis: MeOH: H_2O (70: 30), 6.47 min, 98.1% purity. HRMS (ESI) for $C_{21}H_{16}ClN_7O_3S$ $[M+H]^+$, calcd: 482.0797; found: 482.0793.

3-Chloro-*N*-(4-fluoro-3-(4-(3-methoxy-1*H*-pyrazolo[3,4-*b*]pyridin-5-yl)-1*H*-1,2,3-triazol-1-yl)phenyl)benzenesulfonamide (6d)

Compound **6d** was synthesized from **23c** by a procedure similar to that of **5d**. (Yield: 71% (two steps); TLC: EtOAc: petroleum ether = 1: 2, Rf~0.1). ^{1}H NMR (400 MHz, DMSO-d_6) δ 12.75 (s, 1H), 10.82 (s, 1H), 9.17 (d, J = 2.3 Hz, 1H), 9.11 (d, J = 2.0 Hz, 1H), 8.61 (d, J = 2.0 Hz, 1H), 7.83 (t, J = 1.9 Hz, 1H), 7.77 (t, J = 1.6 Hz, 1H), 7.76-7.73 (m, 1H), 7.67 (dd, J = 6.5, 2.7 Hz, 1H), 7.63 (t, J = 7.9 Hz, 1H), 7.56 (dd, J = 10.4, 9.0 Hz, 1H), 7.30 (ddd, J = 9.0, 4.0, 2.7 Hz, 1H), 4.05 (s, 3H). ^{13}C NMR (101 MHz, DMSO-d_6) δ 155.45, 152.41, 151.83, 149.36, 148.21, 145.73, 141.18, 134.89 (d, J = 2.8 Hz, 1C), 134.51, 133.81,132.07, 126.70, 125.92 (d, J = 4.9 Hz, 1C), 125.27 (d, J = 11.9 Hz, 1C), 123.09 (d, J = 7.7 Hz, 1C), 122.80 (d, J = 5.8 Hz, 1C), 118.91, 118.62 (d, J = 7.9 Hz, 1C), 117.32, 103.79, 56.18. HPLC analysis: MeOH: H_2O (85: 15), 5.41 min; purity: 95.9%. HRMS (ESI) for $C_{21}H_{15}ClFN_7O_3S$ $[M+H]^+$, calcd: 500.0702; found: 500.0700.

3-Chloro-*N*-(2-fluoro-3-(4-(3-methoxy-1*H*-pyrazolo[3,4-*b*]pyridin-5-yl)-1*H*-1,2,3-triazol-1-yl)phenyl)benzenesulfonamide (6e)

Compound **6e** was synthesized from **23d** with by a procedure similar to that of **5d**. (Yield: 69% (two steps); TLC: EtOAc: petroleum ether = 1: 3, Rf~0.1). ^{1}H NMR (400 MHz, DMSO-d_6) δ 12.75 (s, 1H), 10.81 (s, 1H), 9.11 (s, 1H), 9.10 (t, J = 1.5 Hz, 1H), 8.59 (s, 1H), 7.85-7.81 (m, 1H), 7.76 (d, J = 6.3 Hz, 2H), 7.65 (q, J = 8.2 Hz, 2H), 7.42 (t, J = 7.5 Hz, 2H), 4.05 (s, 3H). ^{13}C NMR (101 MHz, DMSO-d_6) δ 155.42, 152.36, 149.58, 148.19, 147.05, 145.45, 142.13, 134.40, 133.67, 131.99, 126.99, 126.58, 125.90, 125.81 (s, 2C), 125.76, 123.25, 123.04, 118.65, 103.77, 56.18. HPLC analysis: MeOH: H_2O (50: 50), 16.52 min; purity: 97.0%. HRMS (ESI) for $C_{21}H_{15}ClFN_7O_3S$ $[M+H]^+$, calcd: 500.0702; found: 500.0702 .

3-Chloro-*N*-(2,6-dichloro-3-(4-(3-methoxy-1*H*-pyrazolo[3,4-*b*]pyridin-5-yl)-1*H*-1,2,3-triazol-1-yl)phenyl)benzenesulfonamide (6f)

Compound **6f** was synthesized from **23e** by a procedure similar to that of **5d** (Yield: 49%, (two steps); TLC: EtOAc: petroleum ether = 1: 1, Rf~0.1). ^{1}H NMR (400 MHz, DMSO-d_6) δ 12.77 (s, 1H), 10.79 (s, 1H), 9.07 (d, J = 2.0 Hz, 1H), 9.05 (s, 1H), 8.55 (d, J = 2.0 Hz, 1H), 7.84 (d, J = 1.9 Hz, 1H), 7.80 (dd, J = 8.7, 2.8 Hz, 2H), 7.75 (d, J = 8.0 Hz, 1H), 7.66 (t, J = 7.9 Hz, 1H), 7.55 (d, J = 8.9 Hz, 1H), 4.05 (s, 3H). ^{13}C NMR (101 MHz, DMSO-d_6) δ 155.46, 152.33, 148.07, 145.28, 142.23, 134.61, 134.52, 133.79, 133.64, 132.03, 130.34, 130.13, 129.52, 129.45, 126.6, 125.79, 125.69, 123.74, 118.50, 103.79, 56.22. HPLC analysis: MeOH: H_2O (70: 30), 9.68 min; purity: 98.4%. HRMS (ESI) for $C_{21}H_{14}Cl_3N_7O_3S$ $[M+H]^+$, calcd: 550.0017; found: 550.0016.

3-Chloro-*N*-(2,4-difluoro-3-(4-(3-methoxy-1*H*-pyrazolo[3,4-*b*]pyridin-5-yl)-1*H*-1,2,3-triazol-1-yl)phenyl)benzamide (6g)

Compound **23a** (70 mg, 0.15 mmol) was dissolved in anhydrous THF (10 mL). To the solution was gradually dropwise added *m*-chlorobenzoyl chloride (32 mg, 0.18 mmol) and triethylamine

(23 mg, 0.23 mmol). The mixture was stirred at rt for 10 min (TLC: EtOAc: petroleum ether = 1:3, Rf~0.3), concentrated in vacuo and purified by column chromatography (20% EtOAc in petroleum ether) to produce 3-chloro-*N*-(2,4-dichloro-3-(4-(3-methoxy-1-(4-methoxybenzyl)-1*H*-pyrazolo[3,4-*b*]pyridin-5-yl)-1*H*-1,2,3-triazol-1-yl)phenyl)benzamide as a white solid (59 mg, yield 64%). ^{1}H NMR (400 MHz, $CDCl_3$) δ 9.03 (d, *J* = 2.1 Hz, 1H), 8.51 (d, *J* = 2.0 Hz, 1H), 8.13 (s, 1H), 7.70 (t, *J* = 1.9 Hz, 1H), 7.59 (d, *J* = 7.7 Hz, 2H), 7.48 (dd, *J* = 8.0, 2.1 Hz, 2H), 7.34 (t, *J* = 8.2 Hz, 3H), 6.85 (d, *J* = 8.4 Hz, 2H), 5.53 (s, 2H), 4.11 (s, 3H), 3.79 (s, 3H). HRMS (ESI) for $C_{30}H_{22}ClF_2N_7O_3$ $[M+H]^+$, calcd: 602.1512; found: 602.1525.

The above product was treated by the general procedure B to afford **6g** as a white solid (Yield: 60%; TLC: MeOH: DCM = 1: 15, Rf~0.3). ^{1}H NMR (400 MHz, DMSO-d_6) δ 12.80 (s, 1H), 10.64 (s, 1H), 9.23 (s, 1H), 9.11 (d, *J* = 2.0 Hz, 1H), 8.60 (d, *J* = 2.0 Hz, 1H), 8.05 (t, *J* = 1.9 Hz, 1H), 7.96 (dt, *J* = 7.9, 1.4 Hz, 1H), 7.91 (dt, *J* = 8.7, 4.3 Hz, 1H), 7.73 (ddd, *J* = 8.1, 2.2, 1.1 Hz, 1H), 7.61 (td, *J* = 9.1, 8.5, 5.3 Hz, 2H), 4.05 (s, 3H). ^{13}C NMR (101 MHz, DMSO-d_6) δ 164.75, 155.43, 152.90, 152.42, 149.71, 148.18, 145.38, 135.73, 133.83, 132.50, 131.13, 130.13 (d, *J* = 9.5 Hz, 1C), 128.09, 127.13, 125.83, 124.56, 123.67 (d, *J* = 11.11 Hz, 1C), 118.47, 115.34 (t, *J* = 15.5 Hz, 1C), 112.81 (d, *J* = 20.4 Hz, 1C), 103.78, 56.18. HPLC analysis: MeOH: H_2O (70: 30), 13.93 min; purity: 99.8%. HRMS (ESI): $C_{22}H_{14}ClF_2N_7O_2$ $[M+H]^+$, calcd: 482.0938; found: 482.0931.

2-(3-Chlorophenyl)-*N*-(2,4-difluoro-3-(4-(3-methoxy-1*H*-pyrazolo[3,4-*b*]pyridin-5-yl)-1*H*-1,2,3-triazol-1-yl)phenyl)acetamide (6h)

Compound **6h** was synthesized from **23a** by a procedure similar to that of **6g** (Yield: 40% (two steps); TLC: MeOH: DCM = 1: 15, Rf~0.3). ^{1}H NMR (400 MHz, DMSO-d_6) δ 12.80 (s, 1H), 10.37 (s, 1H), 9.18 (s, 1H), 9.10 (d, *J* = 2.1 Hz, 1H), 8.59 (d, *J* = 2.0 Hz, 1H), 8.09 (td, *J* = 8.8, 5.7

Hz, 1H), 7.50 (td, *J* = 9.3, 1.8 Hz, 1H), 7.43 (t, *J* = 1.9 Hz, 1H), 7.41-7.29 (m, 3H), 4.05 (s, 3H), 3.80 (s, 2H). ^{13}C NMR (101 MHz, DMSO-d_6) δ 169.82, 155.43, 154.18, 152.43, 151.68, 150.25, 148.17, 145.34, 138.39, 133.31, 130.61, 129.59, 128.42, 127.12, 125.80, 124.48, 124.02 (d, *J* = 10.7 Hz, 1C), 118.47, 115.11 (t, *J* = 14.6 Hz, 1C), 112.59 (d, *J* = 20.1 Hz, 1C), 103.79, 56.15, 42.24. HPLC analysis: MeOH: H_2O (70: 30), 15.58 min; purity 99.3%. HRMS (ESI) for $C_{23}H_{16}ClF_2N_7O_2$ $[M+H]^+$, calcd: 496.1095; found: 496.1088.

1-(3-Chlorophenyl)-3-(2,4-difluoro-3-(4-(3-methoxy-1*H*-pyrazolo[3,4-*b*]pyridin-5-yl)-1*H*-1,2,3-triazol-1-yl)phenyl)urea (6i)

Compound **23a** (150 mg, 0.32 mmol) and 1-chloro-3-isocyanobenzene (59 mg, 0.39 mmol) were dissolved in THF (20 mL), stirred at rt overnight. The mixture was concentrated. The residue was treated with the general procedure B to gave product **6i** as a white solid. (Yield: 57% (two steps); TLC: MeOH/DCM = 1: 10, Rf~0.3). ^{1}H NMR (400 MHz, DMSO-d_6) δ 12.79 (s, 1H), 9.54 (s, 1H), 9.19 (s, 1H), 9.11 (d, *J* = 2.1 Hz, 1H), 9.03 (s, 1H), 8.60 (d, *J* = 2.1 Hz, 1H), 8.31 (td, *J* = 9.0, 5.6 Hz, 1H), 7.75 (t, *J* = 2.0 Hz, 1H), 7.50 (td, *J* = 9.4, 1.8 Hz, 1H), 7.37-7.25 (m, 2H), 7.06 (dt, *J* = 7.7, 1.6 Hz, 1H), 4.06 (s, 3H). ^{13}C NMR (101 MHz, DMSO-d_6) δ 155.42, 152.93, 152.58, 150.12, 148.87, 148.10, 146.36, 145.34, 141.52, 133.69, 130.93, 125.76, 124.47, 124.31, 122.17, 118.39, 118.01, 117.12, 114.89 (t, *J* = 15.6 Hz, 1C), 112.48 (d, *J* = 20.1 Hz, 1C), 103.75, 56.16. HPLC analysis: MeOH: H_2O (85: 15), 6.79 min; purity 99.6%. HRMS (ESI): $C_{22}H_{15}ClF_2N_8O_2$ $[M+H]^+$, calcd: 497.1047; found: 497.1040.

***N*-(2,4-Difluoro-3-(4-(3-methoxy-1*H*-pyrazolo[3,4-*b*]pyridin-5-yl)-1*H*-1,2,3-triazol-1-yl)phenyl)benzenesulfonamide (6j)**

Compound **6j** was synthesized from **23a** by a procedure similar to that of **5d**. (Yield: 53% (two steps); TLC: EtOAc: petroleum ether = 1: 1, Rf~0.15). ^{1}H NMR (400 MHz, DMSO-d_6) δ 12.76 (d, J = 3.1 Hz, 1H), 10.60 (d, J = 3.1 Hz, 1H), 9.08 (d, J = 3.1 Hz, 1H), 9.06 (t, J = 2.5 Hz, 1H), 8.56 (d, J = 2.4 Hz, 1H), 7.82-7.75 (m, 2H), 7.68 (dd, J = 6.6, 2.4 Hz, 1H), 7.65-7.58 (m, 2H), 7.49 (dd, J = 7.7, 4.5 Hz, 2H), 4.05 (d, J = 3.0 Hz, 3H). ^{13}C NMR (101 MHz, DMSO-d_6) δ 155.41, 154.17, 152.40, 151.94, 149.39, 148.15, 145.25, 141.19, 133.11, 129.68, 128.04, 126.94, 125.78, 124.39, 118.45, 115.23 (t, J = 16.6 Hz, 1C), 112.68 (d, J = 20.2 Hz, 1C), 103.76, 56.16. HPLC analysis: MeOH: H_2O (50: 50), 4.26 min; purity 99.6%. HRMS (ESI) for $C_{21}H_{15}F_2N_7O_3S$ $[M+H]^+$, calcd: 484.0998; found: 484.0993.

3-Bromo-*N*-(2,4-difluoro-3-(4-(3-methoxy-1*H*-pyrazolo[3,4-*b*]pyridin-5-yl)-1*H*-1,2,3-triazol-1-yl)phenyl)benzenesulfonamide (6k)

Compound **6k** was synthesized from **23a** with by a procedure similar to that of **5d**. (Yield: 52% (two steps); TLC: EtOAc: petroleum ether = 1: 2, Rf~0.1). ^{1}H NMR (400 MHz, DMSO-d_6) δ 12.77 (s, 1H), 10.74 (s, 1H), 9.10 (s, 1H), 9.07 (d, J = 2.1 Hz, 1H), 8.56 (d, J = 2.1 Hz, 1H), 7.96-7.90 (m, 2H), 7.76 (dt, J = 7.9, 1.4 Hz, 1H), 7.58 (t, J = 7.9 Hz, 1H), 7.51 (d, J = 7.6 Hz, 2H), 4.05 (s, 3H). ^{13}C NMR (101 MHz, DMSO-d_6) δ 155.70, 155.44, 153.18, 152.61, 152.44, 150.04, 148.18, 145.34, 141.97, 136.65, 132.19, 129.93 (d, J = 10.1 Hz, 1C) 129.38, 126.10, 125.85, 124.38, 122.71, 122.26 (d, J = 12.1 Hz, 1C), 118.39, 115.49 (t, J = 16.2 Hz, 1C), 113.21 (d, J = 20.2 Hz, 1C), 103.79, 56.18. HPLC analysis: MeOH: H_2O (60: 40), 4.00 min; purity 98.5%. HRMS (ESI) for $C_{21}H_{14}BrF_2N_7O_3S$ $[M+H]^+$, calcd: 562.0103; found: 562.0102.

3-Cyano-*N*-(2,4-difluoro-3-(4-(3-methoxy-1*H*-pyrazolo[3,4-*b*]pyridin-5-yl)-1*H*-1,2,3-triazol-1-yl)phenyl)benzenesulfonamide (6l)

Compound **6l** was synthesized from **23a** by a procedure similar to that of **5d**. (Yield: 44% (two steps); TLC: MeOH: DCM = 1: 15, Rf~0.15). ^{1}H NMR (400 MHz, DMSO-d_6) δ 12.77 (s, 1H), 10.82 (s, 1H), 9.09 (s, 1H), 9.07 (d, J = 2.1 Hz, 1H), 8.56 (d, J = 2.0 Hz, 1H), 8.23 (d, J = 1.7 Hz, 1H), 8.19 (dt, J = 7.7, 1.3 Hz, 1H), 8.08 (dt, J = 8.0, 1.4 Hz, 1H), 7.84 (t, J = 7.9 Hz, 1H), 7.57-7.45 (m, 2H), 4.05 (s, 3H). ^{13}C NMR (101 MHz, DMSO-d_6) δ 155.56, 155.42, 153.04, 152.41, 148.17, 145.31, 141.53, 137.27, 131.51, 131.42, 130.60, 129.93 (d, J = 10.3 Hz, 1C), 125.85, 124.36, 122.62 (m, 1C), 118.38, 117.89, 115.45 (t, J = 16.9 Hz, 1C), 113.27 (d, J = 3.2 Hz, 1C), 113.08, 103.77, 56.17. HPLC analysis: MeOH: H_2O (60: 40), 11.31 min; purity: 96.5%. HRMS (ESI) for $C_{22}H_{14}F_2N_8O_3S$ $[M+H]^+$, calcd: 509.0950; found: 509.0947.

***N*-(2,4-Difluoro-3-(4-(3-methoxy-1*H*-pyrazolo[3,4-*b*]pyridin-5-yl)-1*H*-1,2,3-triazol-1-yl) phenyl)-3-methoxybenzenesulfonamide (6m)**

Compound **6m** was synthesized from **23a** a procedure similar to that of **5d**. (Yield: 43% (two steps); TLC: EtOAc: petroleum ether = 1: 1, Rf~0.1). ^{1}H NMR (400 MHz, DMSO-d_6) δ 12.77 (s, 1H), 10.60 (s, 1H), 9.10 (s, 1H), 9.06 (d, J = 2.0 Hz, 1H), 8.56 (d, J = 2.1 Hz, 1H), 7.50 (dt, J = 14.9, 8.4 Hz, 3H), 7.36-7.21 (m, 3H), 4.05 (s, 3H), 3.80 (s, 3H). ^{13}C NMR (101 MHz, DMSO-d_6) δ 159.75, 155.53, 152.87, 151.93, 149.56, 148.09, 145.13, 140.53, 131.12, 129.52 (d, J = 9.5 Hz, 1C), 126.25, 124.09, 122.34 (d, J = 11.7 Hz, 1C), 119.63, 119.07, 118.12, 115.02 (t, J = 14.95 Hz, 1C), 113.05 (d, J = 20.5 Hz, 1C), 111.68, 103.90, 56.27, 55.90. HPLC analysis: MeOH: H_2O (60: 40), 6.87 min; purity: 98.9%. HRMS (ESI) for $C_{22}H_{17}F_2N_7O_4S$ $[M+H]^+$, calcd: 514.1104; found: 514.1097.

***N*-(2,4-Difluoro-3-(4-(3-methoxy-1*H*-pyrazolo[3,4-*b*]pyridin-5-yl)-1*H*-1,2,3-triazol-1-yl) phenyl)-3-methylbenzenesulfonamide (6n)**

Compound **6n** was synthesized from **23a** by a procedure similar to that of **5d**. (Yield: 54% (two steps); TLC: EtOAc: petroleum ether = 1: 1, Rf~0.1). ^{1}H NMR (400 MHz, DMSO-d_6) δ 12.77 (s, 1H), 10.55 (s, 1H), 9.10 (s, 1H), 9.06 (d, J = 2.0 Hz, 1H), 8.56 (dd, J = 2.1, 0.7 Hz, 1H), 7.60 (s, 1H), 7.57 (q, J = 2.4, 1.9 Hz, 1H), 7.52-7.46 (m, 4H), 4.05 (s, 3H), 2.38 (s, 3H). ^{13}C NMR (101 MHz, DMSO-d_6) δ 155.44, 152.43, 149.70, 148.16, 145.32, 140.10, 139.61, 134.30, 131.99, 129.72, 129.12, 127.15, 125.82, 124.38, 124.17, 118.40, 115.38 (m, 1C), 113.10 (d, J = 21.5 Hz, 1C), 104.98, 103.78, 56.18, 21.30. HPLC analysis: MeOH: H_2O (50: 50), 10.40 min; purity: 99.0%. HRMS (ESI) for $C_{22}H_{17}F_2N_7O_3S$ $[M+H]^+$, calcd:498.1154; found: 498.1146.

***N*-(2,4-Difluoro-3-(4-(3-methoxy-1*H*-pyrazolo[3,4-*b*]pyridin-5-yl)-1*H*-1,2,3-triazol-1-yl) phenyl)-3-isopropylbenzenesulfonamide (6o)**

Compound **6o** was synthesized from **23a** by a procedure similar to that of **5d**. (Yield: 38% (two steps); TLC: EtOAc: petroleum ether = 1: 2, Rf~0.1). ^{1}H NMR (400 MHz, DMSO-d_6) δ 12.77 (s, 1H), 10.52 (s, 1H), 9.08 (s, 1H), 9.06 (d, J = 2.1 Hz, 1H), 8.57-8.53 (m, 1H), 7.62-7.47 (m, 6H), 3.01-2.92 (m, 1H), 1.17 (d, J = 6.9 Hz, 6H). ^{13}C NMR (101 MHz, DMSO-d_6) δ 155.48, 152.99, 152.33 , 150.34 , 149.82, 148.16, 145.27 , 139.65, 132.09, 129.96, 129.10, 125.95, 124.53, 124.45, 124.29, 118.32 , 115.25, 113.13, 103.81, 56.25, 33.62, 23.89. HPLC analysis: MeOH: H_2O (60: 40), 4.94 min; purity: 96.3%. HRMS (ESI) for $C_{24}H_{21}F_2N_7O_3S$ $[M+H]^+$, calcd: 526.1467; found: 526.1458.

***N*-(2,4-Difluoro-3-(4-(3-methoxy-1*H*-pyrazolo[3,4-*b*]pyridin-5-yl)-1*H*-1,2,3-triazol-1-yl) phenyl)-[1,1'-biphenyl]-3-sulfonamide (6p)**

Compound **6p** was synthesized from **23a** by procedure similar to that of **5d**. (Yield: 46% (two steps); TLC: EtOAc: petroleum ether = 1: 1, Rf~0.3). ^{1}H NMR (400 MHz, DMSO-d_6) δ 12.77 (s,

1H), 10.66 (s, 1H), 9.07 (s, 1H), 9.05 (d, *J* = 2.1 Hz, 1H), 8.54 (d, *J* = 2.0 Hz, 1H), 8.05 (d, *J* = 2.0 Hz, 1H), 8.00 (d, *J* = 7.7 Hz, 1H), 7.76 (d, *J* = 8.0 Hz, 1H), 7.71 (d, *J* = 7.7 Hz, 1H), 7.68 (dd, *J* = 7.4, 1.9 Hz, 2H), 7.58-7.42 (m, 5H), 4.05 (s, 3H). ^{13}C NMR (101 MHz, DMSO-d_6) δ 155.41, 152.88, 152.39, 152.38, 149.71, 148.15, 145.31, 141.75, 140.76, 138.76, 131.96, 130.64, 129.71 (s, 2C), 129.33 (d, *J* = 7.7 Hz, 1C), 128.91, 127.30 (s, 2C), 125.84 (d, *J* = 4 Hz, 1C), 124.87, 124.35, 122.70 (d, *J* = 11.3 Hz, 1C), 118.34, 115.40 (t, *J* = 14.3 Hz, 1C), 113.21 (d, *J* = 18.8 Hz, 1C), 103.76, 56.17. HPLC analysis: MeOH: H_2O (60: 40), 7.52 min; purity: 98.0%. HRMS (ESI) for $C_{27}H_{19}F_2N_7O_3S$ $[M+H]^+$, calcd: 560.1311; found: 560.1305.

_N_-(2,4-Difluoro-3-(4-(3-methoxy-1_H_-pyrazolo[3,4-_b_]pyridin-5-yl)-1_H_-1,2,3-triazol-1-yl) phenyl)naphthalene-2-sulfonamide (6q)

Compound **6q** was synthesized from **23a** by a procedure similar to that of **5d**. (Yield: 48% (two steps); TLC: EtOAc: petroleum ether = 1: 1, Rf~0.1). ^{1}H NMR (400 MHz, DMSO-d_6) δ 12.76 (s, 1H), 10.70 (s, 1H), 9.03 (d, *J* = 2.1 Hz, 1H), 9.02 (s, 1H), 8.52 (d, *J* = 2.1 Hz, 1H), 8.45 (d, *J* = 1.8 Hz, 1H), 8.18 (dd, *J* = 8.3, 5.0 Hz, 2H), 8.06 (d, *J* = 8.1 Hz, 1H), 7.83 (dd, *J* = 8.8, 1.9 Hz, 1H), 7.76-7.66 (m, 2H), 7.52 (q, *J* = 8.1, 7.7 Hz, 1H), 7.44 (t, *J* = 9.2 Hz, 1H), 4.05 (s, 3H). ^{13}C NMR (101 MHz, DMSO-d_6) δ 155.42, 152.90, 152.38, 149.79, 148.13, 145.27, 137.00, 134.85, 132.00, 130.17, 129.82, 129.66, 129.49, 128.37, 128.29, 128.26, 125.84, 124.31,122.60, 122.38, 118.32, 115.35 (t, *J* = 15.0 Hz, 1C), 113.19 (d, *J* = 20.6 Hz, 1C), 103.76, 56.19. HPLC analysis: MeOH: H_2O (85: 15), 4.25 min; purity: 95.9%. HRMS (ESI) for $C_{25}H_{17}F_2N_7O_3S$ $[M+H]^+$, calcd: 534.1154; found: 534.1152.

_N_-(2,4-Difluoro-3-(4-(3-methoxy-1_H_-pyrazolo[3,4-_b_]pyridin-5-yl)-1_H_-1,2,3-triazol-1-yl) phenyl)naphthalene-1-sulfonamide (6r)

Compound **6r** was synthesized from **23a** by a procedure similar to that of **5d**. (Yield: 44% (two steps); TLC: EtOAc: petroleum ether = 1: 1, Rf~0.1). ^{1}H NMR (400 MHz, DMSO-d_6) δ 12.76 (s, 1H), 10.91 (s, 1H), 9.03 (d, J = 2.0 Hz, 1H), 9.02 (s, 1H), 8.70 (d, J = 8.4 Hz, 1H), 8.52 (d, J = 2.0 Hz, 1H), 8.27 (d, J = 8.2 Hz, 1H), 8.16 (dd, J = 7.4, 1.2 Hz, 1H), 8.13-8.09 (m, 1H), 7.76-7.62 (m, 3H), 7.49-7.37 (m, 2H), 4.04 (s, 3H). ^{13}C NMR (101 MHz, DMSO-d_6) δ 155.46, 152.71, 152.34, 149.50, 148.14, 145.25, 135.26, 134.90, 134.25, 129.88, 129.60, 128.95, 128.68, 127.80, 127.59, 125.89, 124.98 , 124.64, 124.26, 122.54, 118.29, 115.24, 113.07 (d, J = 20.9 Hz, 1C), 103.78, 56.22. HPLC analysis: MeOH: H_2O (70: 30), 10.28 min; purity: 96.4%. HRMS (ESI) for $C_{25}H_{17}F_2N_7O_3S$ $[M+H]^+$, calcd: 534.1154; found: 534.1153.

2-Bromo-1-(2,6-difluoro-3-nitrophenyl)ethan-1-one (8)

Concentrated nitric acid (3.2 g, 51 mmol) was added slowly to a solution of 2-bromo-1-(2,6-difluorophenyl)ethan-1-one (10 g, 42.5 mmol) in concentrated sulfuric acid (100 mL) at 0 °C. The mixture was stirred at rt for 2 h (TLC: EtOAc: petroleum ether = 1: 9, Rf~0.4), and poured into crushed ice and further stirred for 30 min, and extracted with EtOAc (150 mL x 3). The organic phase was dried over Na_2SO_4 and evaporated. The residue was purified by flash column chromatography (3% EtOAc in petroleum ether) to obtain **8** as a yellow solid (11g, yield 90%). ^{1}H NMR (400 MHz, DMSO-d_6) δ 8.47 (td, J = 8.9, 5.7 Hz, 1H), 7.56 (td, J = 9.1, 1.8 Hz, 1H), 4.84 (s, 2H). MS (ESI), m/z: 278.0$[M-H]^-$.

3-Methoxy-1-(4-methoxybenzyl)-1*H*-pyrazolo[3,4-b]pyridine-5-carboxylic acid (9)

A mixture of 5-bromo-3-methoxy-1-(4-methoxybenzyl)-1*H*-pyrazolo[3,4-*b*]pyridine (5 g, 14 mmol), HCOOH (2.3 g, 50 mmol), $Pd(OAc)_2$ (94 mg, 0.42 mmol), xantphos (243 mg, 0.42 mmol), dicyclohexylcarbodiimide (DCC) (578 mg, 2.8 mmol) and Et_3N (2.8 g, 28 mmol) was dissolved

in anhydrous DMF (100 mL) and stirred at 100 °C overnight. The mixture was washed with H_2O, acidified with hydrochloric acid (pH 5-6) and filtered. The residue was washed by H_2O to yield **9** as a white solid (4 g, yield 92%). ^{1}H NMR (400 MHz, DMSO-d_6): δ 13.20 (s, 1H), 9.05 (q, J = 2.3 Hz, 1H), 8.55 (q, J = 2.3 Hz, 1H), 7.22 (dt, J = 8.9, 2.3 Hz, 2H), 6.87 (dt, J = 8.7, 2.4 Hz, 2H), 5.48 (t, J = 2.5 Hz, 2H), 4.05-4.00 (m, 3H), 3.73-3.68 (m, 3H). MS (ESI), m/z: 312.1$[M-H]^-$.

2-(2,6-Difluoro-3-nitrophenyl)-2-oxoethyl3-methoxy-1-(4-methoxybenzyl)-1*H*-pyrazolo [3,4-*b*]pyridine-5-carboxylate (10)

A mixture of compound **9** (5.5 g, 17.6 mmol), cesium carbonate (2.9 g, 8.9 mmol) and EtOH (50 mL) was stirred for 2 h at rt. Then the solvent was concentrated in vacuo. Anhydrous DMF (80 mL) and 2-bromo-1-(2,6-difluoro-3-nitrophenyl)ethan-1-one (**8**) (5.9 g, 2.1 mmol) were added. The mixture was further stirred at rt overnight (TLC: EtOAc： petroleum ether = 1: 5, Rf~0.4), washed with H_2O and extracted with EtOAc. The organic phases were washed with brine, dried over anhydrous Na_2SO_4, evaporated and purified by flash column chromatography (15-20% EtOAc in petroleum ether) to give **10** as a yellow solid (4.8 g, yield 52%). ^{1}H NMR (400 MHz, DMSO-d_6) δ 9.10 (d, J = 2.0 Hz, 1H), 8.66 (d, J = 2.0 Hz, 1H), 8.49 (d, J = 5.5 Hz, 1H), 7.61-7.53 (m, 1H), 7.26-7.19 (m, 2H), 6.88 (dd, J = 9.0, 2.3 Hz, 2H), 5.52 (s, 2H), 5.50 (s, 2H), 4.04 (s, 3H), 3.71 (s, 3H). MS (ESI), m/z: 513.0$[M+H]^+$.

2-(3-((3-Chlorophenyl)sulfonamido)-2,6-difluorophenyl)-2-oxoethyl-3-methoxy-1-(4-methoxybenzyl)-1*H*-pyrazolo[3,4-b]pyridine-5-carboxylate (11)

To a solution of **10** (5 g, 9.7 mmol) in H_2O/EtOH (3:7, 100 mL), 0.3 mL concentrated HCl and Fe powder (3.2 g, 58 mmol) were added. The mixture was stirred for 2 h at 70 °C (TLC: EtOAc: petroleum ether = 1: 2, Rf~0.3). The mixture was filtered through celite after cooling, concentrated in vacuo and purified by column chromatography (33% EtOAc in petroleum ether) to obtain 2-(2,6-difluoro-3-nitrophenyl)-2-oxoethyl-3-methoxy-1-(4-methoxybenzyl)-1*H*-pyrazolo[3,4-*b*]pyridine-5 carboxylate as yellow solid (4.3 g, Yield 91%). ^{1}H NMR (400 MHz, DMSO-d_6) δ 9.09 (d, J = 2.2 Hz, 1H), 8.64 (t, J = 2.1 Hz, 1H), 7.25-7.20 (m, 2H), 7.00-6.94 (m, 2H), 6.90-6.85 (m, 2H), 5.52-5.46 (m, 2H), 5.43 (s, 2H), 5.33 (s, 2H), 4.04 (d, J = 2.2 Hz, 3H), 3.71 (d, J = 2.2 Hz, 3H). MS (ESI), m/z: 481.0[M-H]$^-$.

The above product was submitted to the general procedure A to afford **11** as a white solid (Yield 79%; TLC: EtOAc: petroleum ether = 1: 2, Rf~0.4). ^{1}H NMR (400 MHz, DMSO-d_6) δ 10.53 (s, 1H), 9.06 (d, J = 2.0 Hz, 1H), 8.61 (d, J = 2.0 Hz, 1H), 7.78-7.70 (m, 2H), 7.64-7.56 (m, 2H), 7.47-7.39 (m, 1H), 7.28 (dd, J = 9.3, 1.5 Hz, 1H), 7.24-7.19 (m, 2H), 6.89-6.85 (m, 2H), 5.49 (s, 2H), 5.36 (s, 2H), 4.03 (s, 3H), 3.71 (s, 3H). MS (ESI), m/z: 655.0[M-H]$^-$.

3-((3-Chlorophenyl)sulfonamido)-2,6-difluorobenzoic acid (13)

The intermediate methyl 3-((3-chlorophenyl)sulfonamido)-2,6-difluorobenzoate was prepared as a purple solid from **12** (600 mg, 3.2 mmol) according to the general procedure A (1.38 g, yield 84%; TLC: EtOAc: petroleum ether = 1: 3, Rf~0.4). ^{1}H NMR (400 MHz, DMSO-d_6) δ 10.52 (s, 1H), 7.77 (dt, J = 7.2, 2.0 Hz, 1H), 7.73 (t, J = 1.9 Hz, 1H), 7.67-7.59 (m, 2H), 7.46-7.39 (m, 1H), 7.28-7.20 (m, 1H), 3.86 (s, 3H). HRMS (ESI) for $C_{14}H_{10}ClF_2NO_4S$ $[M+H]^+$, calcd: 362.0060; found: 362.0065.

A mixture of methyl 3-((3-chlorophenyl)sulfonamido)-2,6-difluorobenzoate (1.38 g, 3.8 mmol), NaOH (305 mg, 7.6 mmol) and EtOH (50 mL) was stirred for 3 h at rt (TLC: EtOAc: petroleum ether = 1: 1, Rf ~0.1). The solvent was concentrated in vacuo and purified by silica gel column chromatography (10% EtOAc and 0.5% AcOH acid in petroleum ether) to obtain **13** as a white solid (1.2 g, yield 61%): ^{1}H NMR (400 MHz, DMSO-d_6) δ 14.01 (s, 1H), 10.47 (s, 1H), 7.79-7.71 (m, 2H), 7.67-7.59 (m, 2H), 7.35 (td, J = 8.9, 5.7 Hz, 1H), 7.18 (td, J = 9.0, 1.6 Hz, 1H). MS (ESI) m/z: 346.0[M-H]$^-$.

3-Methoxy-1-(4-methoxybenzyl)-1*H*-pyrazolo[3,4-*b*]pyridine-5-carbohydrazide (14)

A mixture of **9** (5.8 g, 18.5 mmol) and K_2CO_3 (3.8 g, 27.8 mmol) was dissolved in DMF (100 mL) and CH_3I (6.6 g, 46.3 mmol) was added slowly to the solution. The mixture was stirred for 4 h at rt (TLC: EtOAc: petroleum ether = 1: 10, Rf~0.3), poured into H_2O, extracted with EtOAc, washed with brine, dried over anhydrous Na_2SO_4, then evaporated and purified by flash column chromatography (10% EtOAc in petroleum ether) to produce methyl 3-methoxy-1-(4-methoxybenzyl)-1*H*-pyrazolo[3,4-*b*]pyridine-5-carboxylate as a white solid (5.6 g, yield 88%). ^{1}H NMR (400 MHz, DMSO-d_6) δ 9.06 (d, 1H), 8.59 (d, 1H), 7.22 (d, J = 6.4, 3.0 Hz, 2H), 6.90-6.84 (d, 2H), 5.50-5.44 (s, 2H), 4.02 (s, J = 6.6, 3.7 Hz, 3H), 3.89 (s, J = 6.6, 3.6 Hz, 3H), 3.70 (s, J = 6.3, 3.7 Hz, 3H). HRMS (ESI) for $C_{17}H_{17}N_3O_4$ [M+H]$^+$, calcd: 328.1292; found: 328.1293.

Hydrazine hydrate (45%, 5.5 g, 49.5 mmol) was added slowly to the above product (5.4 g, 16.5 mmol) in EtOH (80 mL). The mixture was stirred at 86 °C overnight (TLC: MeOH: DCM = 1: 15, Rf~0.4), cooled and filtered. The residue was washed with EtOH to give the intermediate **14** (3.3 g, yield 61%) as a white solid. ^{1}H NMR (400 MHz, DMSO-d_6) δ 9.89 (s, 1H), 8.98 (d, J = 2.1 Hz,

1H), 8.54 (d, *J* = 2.1 Hz, 1H), 7.23-7.16 (m, 2H), 6.89-6.83 (m, 2H), 5.46 (s, 2H), 4.53 (s, 2H), 4.02 (s, 3H), 3.71 (s, 3H). HRMS (ESI) for $C_{16}H_{17}N_5O_3$ $[M+H]^+$, calcd: 328.1404; found: 328.1393.

3-Chloro-*N*-(2,4-difluoro-3-(2-(3-methoxy-1-(4-methoxybenzyl)-1*H*-pyrazolo[3,4-*b*] pyridine-5-carbonyl)hydrazine-1-carbonyl)phenyl)benzenesulfonamide (15)

A mixture of **14** (320 mg, 0.98 mmol), 3-((3-chlorophenyl)sulfonamido)-2,6-difluorobenzoic acid **13** (407 mg, 1.17 mmol), DIEA (190 mg, 1.17 mmol) and HATU (446 mg, 1.47 mmol) was dissolved in DCM (50 mL). The mixture was stirred for 4 h at rt (TLC: MeOH: DCM ether = 1: 15, Rf~0.5). The mixture was filtered and washed with DCM to afford **15** as a white solid (592 mg, yield 92%). ^{1}H NMR (400 MHz, DMSO-d_6) δ 10.84 (s, 1H), 10.80 (s, 1H), 10.51 (s, 1H), 9.05 (t, *J* = 1.7 Hz, 1H), 8.67 (t, *J* = 1.7 Hz, 1H),7.81-7.74 (m, 2H), 7.71-7.60 (m, 2H), 7.34 (td, *J* = 8.8, 5.8 Hz, 1H), 7.20 (dd, *J* = 15.6, 8.4 Hz, 3H), 6.90-6.85 (m, 2H), 5.49 (s, 2H), 4.04 (d, *J* = 1.4 Hz, 3H), 3.71 (d, *J* = 1.4 Hz, 3H). HRMS (ESI) for $C_{29}H_{23}ClF_2N_6O_6S$ $[M-H]^-$, calcd: 655.0984; found: 655.0975.

3-Chloro-*N*-(3-cyano-2,4-difluorophenyl)benzenesulfonamide (17)

Compound **17** was synthesized from 3-amino-2,6-difluorobenzonitrile **16** (1.3 g, 8.4 mmol) according to the general procedure A as a yellow solid (1.96 g, yield 71%, TLC: EtOAc: petroleum ether = 1: 1, Rf~0.8 in). ^{1}H NMR (400 MHz, DMSO-d_6) δ 10.72 (s, 1H), 7.82-7.74 (m, 2H), 7.68-7.56 (m, 3H), 7.40 (td, *J* = 8.9, 1.5 Hz, 1H). MS (ESI) m/z: 327.0$[M-H]^-$.

(*Z*)-3-((3-Chlorophenyl)sulfonamido)-2,6-difluoro-*N*'-hydroxybenzimidamide (18)

17 (800 mg, 2.4 mmol), sodium bicarbonate (1 g, 12.2 mmol) and hydroxylamine hydrochloride (848 mg, 12.2 mmol) were dissolved in EtOH (100 mL) and stirred at 85 °C for 3 h (TLC: EtOAc:

petroleum ether = 1: 1, Rf~0.4). The mixture was filtered, washed with EtOH, and concentrated in vacuo to give **18** as a yellow solid (830 mg, yield 96%). ^{1}H NMR (400 MHz, DMSO-d_6) δ 10.39 (s, 1H), 9.60 (d, J = 2.0 Hz, 1H), 7.80-7.74 (m, 2H), 7.69-7.58 (m, 2H), 7.25 (tdd, J = 8.7, 5.9, 1.8 Hz, 1H), 7.10 (td, J = 8.9, 1.7 Hz, 1H), 5.95 (s, 2H). HRMS (ESI) for $C_{13}H_{10}ClF_2N_3O_3S$ $[M+H]^+$, calcd: 362.0172.0448; found: 362.0162.

(*Z*)-3-((3-Chlorophenyl)sulfonamido)-2,6-difluoro-*N*'-((3-methoxy-1-(4-methoxybenzyl)-1*H*-pyrazolo[3,4-*b*]pyridine-5-carbonyl)oxy)benzimidamide (19)

A mixture of **9** (100 mg, 0.32 mmol), **18** (116 mg, 0.32 mmol), Et_3N (49 mg, 0.48 mmol) and HATU (182.7 mg, 0.48 mmol) was dissolved in DCM (50 mL). The mixture was stirred at rt for 4 h (TLC: EtOAc: petroleum ether = 1:1, Rf~0.3), concentrated in vacuo and purified by column chromatography (40% EtOAc in petroleum ether) to give **19** as a yellow solid (126 mg, yield 60%). ^{1}H NMR (400 MHz, DMSO-d_6) δ 10.51 (s, 1H), 9.20 (d, J = 2.1 Hz, 1H), 9.01 (d, J = 2.1 Hz, 1H), 7.85-7.81 (m, 1H), 7.77 (d, J = 7.9 Hz, 1H), 7.70 (d, J = 7.8 Hz, 1H), 7.63 (t, J = 7.8 Hz, 1H), 7.48-7.29 (m, 3H), 7.27-7.17 (m, 3H), 6.88 (d, J = 8.7 Hz, 2H), 5.49 (s, 2H), 4.05 (s, 3H), 3.72 (s, 3H).. HRMS (ESI) for $C_{29}H_{23}ClF_2N_6O_6S$ $[M-H]^-$, calcd: 655.0984; found: 655.0983.

2-Azido-1,3-difluoro-4-nitrobenzene (21a)

2,6-difluoro-3-nitroaniline **20a** (10 g, 57.5 mmol) was suspended in TFA (400 mL) at 0 °C. $NaNO_2$ (6 g, 86 mmol) was added in small portions with care because of the release of toxic gas and the reaction mixture was stirred for 30 min at 0 °C. Then NaN_3 (7.5 g, 115 mmol) was added in small portions. The mixture was stirred for 2 h at 0 °C (TLC: EtOAc: petroleum ether = 1: 10; Rf~0.8). The solution was extracted with EtOAc, washed with brine, dried over Na_2SO_4,

evaporated and purified by flash column chromatography (3% EtOAc in petroleum ether) to produce **21a** as a dark red solid (11 g, yield 95%). ^{1}H NMR (400 MHz, DMSO-d_6) δ 8.05 (ddd, J = 9.5, 8.4, 5.5 Hz, 1H), 7.47 (td, J = 9.8, 2.0 Hz, 1H).

1-Azido-3-nitrobenzene (21b)

Compound **21b** was synthesized from 3-nitroaniline **20b** with a procedure similar to that of **21a** (yield 96%; TLC: EtOAc: petroleum ether = 1: 9, Rf~0.7). ^{1}H NMR (400 MHz, DMSO-d_6) δ 8.04 (dd, J = 8.1, 2.2 Hz, 1H), 7.88 (q, J = 2.0 Hz, 1H), 7.70 (td, J = 8.1, 1.5 Hz, 1H), 7.64-7.60 (m, 1H).

2-Azido-1-fluoro-4-nitrobenzene (21c)

Compound **21c** was synthesized from 2-fluoro-5-nitroaniline **20c** with a procedure similar to that of **21a** (yield 95%; TLC: EtOAc: petroleum ether = 1: 10, Rf~0.8). ^{1}H NMR (400 MHz, DMSO-d_6) δ 8.18-8.05 (m, 2H), 7.62 (dd, J = 10.4, 9.0 Hz, 1H).

1-Azido-2-fluoro-3-nitrobenzene (21d)

Compound **21d** was synthesized from 2-fluoro-3-nitroaniline **20d** with a procedure similar to that of **21a** (yield 95%; TLC: EtOAc: petroleum ether = 1: 10, Rf~0.7). ^{1}H NMR (400 MHz, DMSO-d_6) δ 8.08 (td, J = 8.2, 1.5 Hz, 2H), 7.40 (t, J = 8.2 Hz, 1H).

2-Azido-1,3-dichloro-4-nitrobenzene (21e)

Compound **21e** was synthesized from 2,6-dichloro-3-nitroaniline **20e** with a procedure similar to that of **21a** (yield 84%; TLC: EtOAc: petroleum ether = 1: 10; Rf~0.8). ^{1}H NMR (400 MHz, CDCl3) δ 7.62 (d, J = 8.8 Hz, 1H), 7.48 (d, J = 8.8 Hz, 1H).

5-Ethynyl-3-methoxy-1-(4-methoxybenzyl)-1*H*-pyrazolo[3, 4-*b*]pyridine (22a)

The synthesis of compound **22a** was described in our previous study[17].

2,4-Difluoro-3-(4-(3-methoxy-1-(4-methoxybenzyl)-1*H*-pyrazolo[3,4-*b*]pyridin-5-yl)-1*H*-1,2,3-triazol-1-yl)aniline (23a)

A mixture of **22a** (10 g, 34.1 mmol), **21a** (7.5 g, 37.5 mmol), sodium ascorbate (13.5 g, 68.2 mmol) and copper (II) sulfate pentahydrate (8.5 g, 34.1 mmol) were dissolved in a solution of H_2O: *t*-BuOH (1: 1) (150mL), then stirred at 95 °C for 3 h (TLC: EtOAc: petroleum ether = 1: 2, Rf~0.4). Then, concentrated HCl (0.3 mL) and Fe powder (5.7 g, 102.3 mmol, 3 eq) were added. The whole mixture was further stirred at 70 °C for 2 h (TLC: EtOAc: petroleum ether = 1: 2, Rf~0.3), filtered through celite after cooling, acidified with HCl (pH 6-7) and extracted with EtOAc. The organic layer was washed with brine, dried over Na_2SO_4, concentrated in vacuo and purified by column chromatography (25-33% EtOAc in petroleum ether) to obtain **23a** as a yellow solid (9.5 g, yield 60%). ^{1}H NMR (400 MHz, DMSO-d_6) δ 9.15 (d, J = 2.0 Hz, 1H), 9.13 (s, 1H), 8.59 (d, J = 2.0 Hz, 1H), 7.26-7.21 (m, 2H), 7.17 (dd, J = 9.3, 1.7 Hz, 1H), 7.02 (td, J = 9.4, 5.4 Hz, 1H), 6.90-6.85 (m, 2H), 5.54 (s, 2H), 5.48 (s, 2H), 4.04 (s, 3H), 3.71 (s, 3H). MS (ESI) m/z: 462.0[M-H]$^-$.

3-(4-(3-Methoxy-1-(4-methoxybenzyl)-1*H*-pyrazolo[3,4-*b*]pyridin-5-yl)-1*H*-1,2,3-triazol-1-yl)aniline (23b)

Compound **23b** was synthesized from **21b** and **22a** with a procedure similar to that of **23a** (yield 62%; TLC: EtOAc: petroleum ether = 1:2, Rf~0.3). ^{1}H NMR (400 MHz, DMSO-d_6) δ 9.26 (s, 1H), 9.15 (d, J = 2.0 Hz, 1H), 8.59 (d, J = 2.0 Hz, 1H), 7.28-7.19 (m, 3H), 7.14 (t, J = 2.2 Hz, 1H), 6.97

(ddd, *J* = 7.9, 2.1, 0.9 Hz, 1H), 6.92-6.84 (m, 2H), 6.68 (ddd, *J* = 8.1, 2.2, 0.9 Hz, 1H), 5.60 (s, 2H), 5.48 (s, 2H), 4.04 (s, 3H), 3.71 (s, 3H). MS (ESI) m/z: 428.2[M+H]$^+$.

4-Fluoro-3-(4-(3-methoxy-1-(4-methoxybenzyl)-1*H*-pyrazolo[3,4-*b*]pyridin-5-yl)-1*H*-1,2,3-triazol-1-yl)aniline (23c)

Compound **23c** was synthesized from **21c** and **22a** by a procedure similar to that of **23a** (yield 58%; TLC: EtOAc: petroleum ether = 1: 3, Rf~0.3). ^{1}H NMR (400 MHz, DMSO-d_6) δ 9.17 (d, *J* = 2.0 Hz, 1H), 9.12 (d, *J* = 2.2 Hz, 1H), 8.62 (d, *J* = 2.0 Hz, 1H), 7.27-7.20 (m, 3H), 7.01 (dd, *J* = 6.3, 2.8 Hz, 1H), 6.90-6.85 (m, 2H), 6.73 (ddd, *J* = 8.9, 4.0, 2.8 Hz, 1H), 5.47 (d, *J* = 2.8 Hz, 4H), 4.04 (s, 3H), 3.71 (s, 3H). MS (ESI) m/z: 446.2[M+H]$^+$.

2-Fluoro-3-(4-(3-methoxy-1-(4-methoxybenzyl)-1*H*-pyrazolo[3,4-*b*]pyridin-5-yl)-1*H*-1,2,3-triazol-1-yl)aniline (23d)

Compound **23d** was synthesized from **21d** and **22a** by a procedure similar to that of **23a**. Yield 58%; TLC: EtOAc: petroleum ether = 1: 2, Rf~0.25. ^{1}H NMR (400 MHz, DMSO-d_6) δ 9.18 (d, *J* = 2.0 Hz, 1H), 8.92 (s, 1H), 8.58 (d, *J* = 2.0 Hz, 1H), 7.26-7.21 (m, 2H), 7.18 (d, *J* = 8.1 Hz, 1H), 6.97-6.92 (m, 1H), 6.91-6.85 (m, 3H), 5.54 (s, 2H), 5.48 (s, 2H), 4.03 (s, 3H), 3.71 (s, 3H). MS (ESI) m/z: 446.0[M+H]$^+$.

2,4-Dichloro-3-(4-(3-methoxy-1-(4-methoxybenzyl)-1*H*-pyrazolo[3,4-*b*]pyridin-5-yl)-1*H*-1,2,3-triazol-1-yl)aniline (23e)

Compound **23e** was synthesized from **21e** and **22a** by a procedure similar to that of **23a** (yield 52%; TLC: EtOAc: petroleum ether = 1: 2, Rf~0.3). ^{1}H NMR (400 MHz, DMSO-d_6) δ 9.16 (d, *J* = 2.0 Hz, 1H), 9.07 (s, 1H), 8.59 (d, *J* = 2.0 Hz, 1H), 7.44 (d, *J* = 9.0 Hz, 1H), 7.25-7.20 (m, 2H),

7.06 (d, *J* = 8.9 Hz, 1H), 6.90-6.85 (m, 2H), 6.10 (s, 2H), 5.48 (s, 2H), 4.03 (s, 3H), 3.71 (s, 3H). HRMS (ESI) for $C_{23}H_{19}Cl_2N_7O_2$ $[M+H]^+$, calcd: 496.1050; found: 496.1047.

5-(1-(3-Amino-2,6-difluorophenyl)-1*H*-1,2,3-triazol-4-yl)pyridin-2-amine (23f)

Compound **23f** was synthesized from 5-ethynylpyridin-2-amine **22b** and **21a** by a procedure similar to that of **23a** (yield54%; TLC: MeOH: DCM ether = 1: 15, Rf~0.4). ^{1}H NMR (400 MHz, DMSO-d_6) δ 8.83 (d, *J* = 1.9 Hz, 1H), 8.48 (s, 1H), 7.88 (dd, *J* = 8.6, 2.2 Hz, 1H), 7.15 (td, *J* = 9.3, 4.5 Hz, 1H), 7.00 (qd, *J* = 9.4, 8.5, 3.7 Hz, 1H), 6.56 (d, *J* = 8.6 Hz, 1H), 6.22 (s, 2H), 5.53 (s, 2H). MS (ESI) m/z: 289.1$[M+H]^+$.

5-(1-(3-Amino-2,6-difluorophenyl)-1*H*-1,2,3-triazol-4-yl)pyrimidin-2-amine (23g)

Compound **23g** was synthesized from 5-ethynylpyrimidin-2-amine **22c** and **21a** by a procedure similar to that of **23a** (yield50%; TLC: MeOH: DCM ether = 1: 15, Rf~0.4). ^{1}H NMR (400 MHz, DMSO-d_6) δ 8.91 (s, 1H), 8.76 (s, 2H), 7.16 (td, *J* = 9.3, 1.8 Hz, 1H), 7.01 (dt, *J* = 9.4, 4.7 Hz, 1H), 6.97 (s, 2H), 5.54 (s, 2H). MS (ESI) m/z: 288.0$[M-H]^-$.

Molecular Modeling. The computational docking studies were performed in Maestro 11.5 (version 11.5.001, Schrödinger, New York, USA). The ZAK (PDB: 5X5O) and B-Raf^{V600E} (PDB:3OG7) protein structures were prepared with "Protein Preparation Wizard" option by adding hydrogens and removing water molecules. Compound **5d** was built by in LigPrep module using OPLS-2005 force field. The docking program was performed in Glide module in in Maestro 11.5. The grid-enclosing boxes were placed on the centroid of the 0LI based on the crystal structures of ZAK and B-Raf^{V600E}, respectively. Standard precision (SP) approach in Glide module was applied with other setting by default parameters.

***In Vitro* Kinase Assay.** The *in vitro* ZAK and B-Raf^{V600E} kinases assay were carried out as our previous described. [17]

KINOMEscan™. The KINOMEscan profiling and the binding constant (K_d) of ZAK and other potential "off-targets" were carried out as our previous described.[17] Detail data for the 468 kinase KINOMEscan are in Supporting Information.

Western Blot Analysis. Proteins samples (30-50 µg) were separated by 10-12% sodium dodecyl sulfate polyacrylamide gel electrophoresis (SDS-PAGE) and transferred to a polyvinylidene difluoride (PVDF) membrane at 100 V. Following transfer, membranes were then blocked in blocking buffer (5% skim milk in TBST) for 1 h at rt and thereafter washed thrice with TBST 15 min each and finally incubated with specific primary antibodies against JNK (sc-571), p-JNK (sc-6254), c-Jun (sc-1694), p-c-Jun (sc-16312-R), p38 (sc-33688), GATA-4 (sc-25310), p-GATA-4(sc-32823), α-Tubulin (sc-5286), β-actin (sc-47778) ANP (sc-20158) from Santa Crux Biotechnology, Inc., Dallas, Texas, USA, p-p38 (9211) from Cell Signalling Technology, Ozyme, St Quentin en Yvelines, France) and ZAK (H00051776) from Abcam, Cambridge, UK) (1:1000 dilution) overnight at 4 ºC. Subsequent to these steps, usual washing step with TBST for 15 min each were performed and finally the membranes were incubated with Goat anti-mouse (sc-2005, 1:10000), goat anti-rabbit (sc-2004, 1:10000) and donkey anti-goat (sc-2056, 1:10000) secondary antibodies (IgG conjugated to HRP) for 2h at RT. Protein levels were quantified with LAS 3000 image analyzer (Fujifilm, Tokyo, Japan)

Construction of Tet-on Gene Expression System. The Tet-on ZAKα expression system was established by transfecting pTRE-ZAKα in H9c2 cells as described previously.[20] In brief, pTRE-ZAKα was transfected in cells containing pTet-on plasmid that constitutively expresses rtTA

protein that binds to and activates the promoter on pTRE plasmid in the presence of doxycycline or tetracycline to trigger ZAKα expression. In this way, H9c2 cells were created such that their ZAKα expression was control by Dox.

Actin-fluorescence (rhodamine–phalloidin) staining. The H9c2 cells were fixed using 4% paraformaldehyde, permeabilized with 0.5% Triton X-100 for 10 min and were blocked with 2% goat serum (in PBS) at 37 °C for 30 min. The actin filaments were stained with rhodamine-labeled phalloidin (Invitrogen, Carlsbad, CA, USA) following the manufacturer's protocol and photographed using a fluorescence microscope (Olympus, Tokyo, Japan). For cell size determination thirty cells in each well were counted and treated as an independent experiment; three independent experiments were performed in each condition.

Immunofluorescence staining. H9c2 cells were cultured in chambered slides and were fixed, permeabilized and blocked using methods similar to those performed for Actin Staining. The cells were incubated overnight at 4 °C with primary antibodies (1:400 diluted with 1% BSA in PBS). The cells were then washed with PBS and incubated in diluted secondary antibody and incubated in dark at 37 °C for 1 h. The cells were then stained with DAPI to counterstain the nucleus.

Animal Experiments. All experimental procedures with animals conform to the Guidelines for the Care and Use of Laboratory Animals (National Institutes of Health Publication No. 85-23, revised 1996) and were executed under a strict protocol approved by the Animal Research Committee of China Medical University, Taichung, Taiwan. Age-matched spontaneously hypertensive rats (SHR) and normotensive control Wistar–Kyoto rats (WKY) were purchased from BioLASCO, Taipei, Taiwan (ROC). The rats were housed in the animal facility centre at China Medical University, Taichung, Taiwan under a 12-hour light/dark cycle with free access of

food and water *ad libitum*. The animals were randomly divided into following groups: control WKY rats supplemented with PBS, control SHR rats supplemented with PBS, and SHR rats supplemented with low dose of ZAK inhibitor (**6p**: 2.5 mg/kg body weight) and SHR rats supplemented with high dose of ZAK inhibitor (**6p**: 10 mg/kg body weight). Each group consisted of six male 12-week-old animals. The dosages were administered every day per week for a time interval of 8 weeks through oral gavages. All necessary procedures were undertaken to reduce pain to the animals. At the end of the experiments, the animals were euthanized in a prefilled CO_2 chamber with 100% CO_2 and sacrificed through decapitation. The heart tissues were collected, residual blood was washed off with cold 1×PBS, the left ventricle tissue sections were isolated from whole heart tissue and stored at -80 °C prior to protein extraction.

Protein Extraction. Tissue lysates were prepared by homogenization in ice cold modified RIPA buffer (0.2% sodium deoxycholate, 50 mM Tris -HCl, pH 7.4, 1% Triton X-100, 0.2% sodium dodecylsulfate, 1 mM phenylmethylsulfonyl fluoride, 1 mM sodium ethylenediaminetetraacetate, 5 μg/ml of leupeptin and 5 μg/ml of aprotinin). Following homogenization, cell debris were removed by centrifugation at 14,000×g at 4°C for 30 min and thereafter stored at -80 °C. Protein concentration was determined with Bio-Rad protein assay. The lysate was boiled 1 x SDS sample buffer (12.5% glycerol, 50 mM Tris -HCl pH 6.8, 0.01% bromophenol blue, 1% SDS) containing 5% β-mercaptoethanol for 5 min at 95°C.

Hematoxylin and Eosin Staining. The heart tissues were fixed with 10% formalin, treated with series of alcohol gradient (75%, 85%, 90%, and 100% liquor, 5 min each) and embedded in paraffin wax. Paraffin embedded sections were cut into 0.2 m-thick slices and deparaffinized by submersion in xylene solution. Following this, the tissue sections were stained with H&E

following recommended procedures in previous studies.[17] Micrographs were acquired at 400 X magnification under a light microscope (Olympus Microscope CKX53, Tokyo, Japan).

Determination of Pharmacokinetic Parameters in Rats. Compound **6p** (10.01mg) was dissolved in mixed solvents (0.500 mL DMSO, 1.000mL solutol and 8.50 mL saline) for intravenous injection and oral dosing with a final concentration of 1.0 mg/mL. SD rats (male, 3 animals per group) weighing 180~220g were injected **6p** intravenously and oral at a dose of 2.5 mg/kg and 10 mg/kg, respectively. After administration, 0.25 mL of the orbital blood was taken at 0.083 h, 0.25 h, 0.5 h, 1.0 h, 2.0 h, 3.0 h, 4.0 h, 6.0 h, 8.0 h, 24.0 h for injection group, and 0.25 h, 0.5 h, 1.0 h, 2.0 h, 3.0 h, 4.0 h, 6.0 h, 8.0 h, 24.0 h for oral group, respectively. Samples were stored at -80 °C until shipment to the analytical laboratory and tested by HPLC/MS using propranolol as internal standard to measure the compound concentration in the blood. The pharmacokinetic parameters were calculated using DAS (Drug and Statistics) 2.0 software (Mathematical Pharmacology Professional Committee of China, Shanghai, China).

Crystallization and Structure Determination.

The ZAK 5-309 proteins were prepared as previously described.[17] For co-crystallization process, 100mM **6k** solution was added to 20mg/mL ZAK protein solution to achieve the final concentration of 2 mM compound. The mixture was incubated on ice for 2 hours and then applied to crystallization. The crystallization reservoir solution was 0.1M Bis-Tris pH 5.5, 25% PEG3350, 0.2M NaCl. The diffraction data were collected at beamline BL19U1, Shanghai Synchrotron Radiation Facility (SSRF) at 100K. The X-ray wavelength for data collection was 0.97861Å and the diffraction data were processed with HKL3000.[22] The structure was solved as similar previously described.[17] See details in Supporting information.

ASSOCIATED CONTENT

Supporting Information. The selectivity profiling study of compound **6p**, crystal data collection and refinement statistics of **6k**, the ^{1}H and ^{13}C NMR spectra of compounds **5a-5d** and **6a-6r**, HPLC conditions and traces for the representative compounds and Molecular Formula Strings (CSV). All the materials are available free of charge via the Internet at http://pubs.acs.org.

AUTHOR INFORMATION

Corresponding Author

*yunch@hsc.pku.edu.cn (C.H. Y.)

*cyhuang@mail.cmu.edu.tw (C.Y. H.)

*dingke@jnu.edu.cn (K. D.)

*luxy2016@jnu.edu.cn (X.Y. L.), phone: +86-20-85223259.

Author Contributions

#Jianzhang Yang , Marthandam Asokan Shibu and Lulu Kong contributed equally to this work.

Notes

The authors declare no competing financial interest.

ACKNOWLEDGMENT

The work was supported by National Natural Science Foundation of China (81673285, 81874285 and 81820108029), Guangdong Provincial Science and Technology Project

(2018A050506043), Guangdong Natural Science Funds (2015A030306042) and Guangzhou City Key Laboratory of Precision Chemical Drug Development (201805010007).

ABBREVIATIONS

ZAK, leucine-zipper and sterile-α motif kinase; HCM, hypertrophic cardiomyopathy; SHR, spontaneous hypertensive rat; ANF, atrial natriuretic factor; LVH, left ventricular hypertrophy; BNP, brain natriuretic peptide; MLK, mixed-lineage kinase; MHC, myosin heavy chain; JNK, c-Jun N-terminal protein kinase; DN, dominant negative; SAR, structure activity relationships; HB, hydrogen bonds; BLK, B lymphoid tyrosine kinase; FLT3, Fms-like tyrosine kinase 3; LIMK1, LIM domain kinase 1; LIMK2, LIM domain kinase 2; LCK, lymphocyte-specific protein tyrosine kinase; RIPK2, receptor-interacting serine/threonine-protein kinase 2; Dox, doxycycline; PK, pharmacokinatics; AUC, area under curve; SD, sprague-Dawley; MBP, myelin basic protein; MAPK, mitogen activated protein kinase; WKY, Wistar–Kyoto rats; SDS, sodium dodecylsulfate; H&E, hematoxylin and eosin; SSRF, synchrotron radiation facility; WH, whole heart; LV, the left ventricular.

REFERENCES

1. Sen-Chowdhry, S.; Jacoby, D.; Moon, J. C.; McKenna, W. J. Update on hypertrophic cardiomyopathy and a guide to the guidelines. *Nat. Rev. Cardiol.* **2016**, *13*, 651-675.

2. Maron B. J. Hypertrophic cardiomyopathy: a systematic review. *JAMA*, **2002**, 287, 1308-1320.

3. Sugden, P.H.; Clerk, A. Cellular mechanisms of cardiac hypertrophy. *J. Mol. Med.* **1998**, *76*, 725-746.

4. Hanford, D. S.; Thuerauf, D. J.; Murray, S. F.; Glembotski, C. C. Brain natriuretic peptide isinduced by α1-adrenergic agonists as a primary response gene in cultured rat cardiac myocytes. *J. Biol. Chem*. **1994**, *269*, 26227-26233.

5. Marsiglia, J. D. C.; Pereira, A. C. Hypertrophic cardiomyopathy: how do mutations lead to disease? *Arq. Bras. Cardiol.* **2014**, *102*, 295–304.

6. Robert-Paganin J, Auguin D, Houdusse A. Hypertrophic cardiomyopathy disease results from disparate impairments of cardiac myosin function and auto-inhibition. *Nat. Commu.* **2018**, 9, 4019-4032.

7. Hamada, M.; Ikeda, S.; Shigematsu, Y. Advances in medical treatment of hypertrophiccardiomyopathy. *J. Cardiol.* **2014**, *64*, 1-10.

8. Liu, T.C.; Huang, C.J.; Chu, Y.C.; Wei, C.C.; Chou, C.C.; Chou, M.Y.; Chou, C.K.; Yang, J.J. Cloning and expression of ZAK, a mixed lineage kinase-like protein containing a leucine-zipper and a sterile-alpha motif. *Biochem. Biophys. Res. Commun.* **2000**, *274*, 811-816.

9. Chang, Y.; Zhang, Q. W.; Li, Z. Q.; Ding, K.; Lu, X. Y. Leucine-zipper and sterile-*α* motif kinase (ZAK): a potential target for drug discovery. *Curr. Med. Chem.* **2016**, *23*, 3801-3812.

10. Huang, C. Y.; Chueh, P. J.; Tseng, C. T.; Liu, K. Y.; Tsai, H. Y.; Kuo, W. W.; Chou, M. Y.; Yang, J. J. ZAK re-programs atrial natriuretic factor expression and induces hypertrophic growth in H9c2 cardiomyoblast cells. *Biochem. Biophys. Res. Commun.* **2004**, *324*, 973-980.

11. Hsieh, Y. L.; Tsai, Y. L.; Shibu, M. A.; Su, C. C.; Chung, L. C.; Pai, P.; Kuo, C. H.; Yeh, Y. L.; Viswanadha, V. P.; Huang, C. Y. ZAK induces cardiomyocyte hypertrophy and brain

natriuretic peptide expression via p38/JNK signalling and GATA4/c-Jun transcriptional factor activation. *Mol. Cell. Biochem.* **2015**, *405*, 1-9.

12. Huang, C. Y.; Kuo, W. W.; Chueh, P. J.; Tseng, C. T.; Chou, M. Y.; Yang, J. J. Transforming growth factor-*β* induces the expression of ANF and hypertrophic growth in cultured cardiomyoblast cells through ZAK. *Biophys. Res. Commun*. **2004**, *324*, 424-431.

13. Mathea, S.; Abdul Azeez, K. R.; Salah, E.; Tallant, C.; Wolfreys, F.; Konietzny, R.; Fischer, R.; Lou, H. J.; Brennan, P. E.; Schnapp, G.; Pautsch, A.; Kessler, B. M.; Turk, B. E.; Knapp, S. Structure of the human protein kinase ZAK in complex with vemurafenib. *ACS Chem. Biol.* **2016**, *11*, 1595−1602.

14. Vin, H.; Ching, G.; Ojeda, S. S.; Adelmann, C. H.; Chitsazzadeh, V.; Dwyer, D. W.; Ma, H.; Ehrenreiter, K.; Baccarini, M.; Ruggieri, R.; Curry, J. L.; Ciurea, A. M.; Duvic, M.; Busaidy, N. L.; Tannir, N. M.; Tsai, K. Y. Sorafenib suppresses JNK-dependent apoptosis through inhibition of ZAK. *Mol. Cancer Ther*. **2014**, *13*, 221−229.

15. Manley, P. W.; Drueckes, P.; Fendrich, G.; Furet, P.; Liebetanz, J.; Baron, G. M.; Mestan, J.; Trappe, J.; Wartmann, M.; Fabbro, D. Extended kinase profile and properties of the protein kinase inhibitor nilotinib. *Biochim. Biophys. Acta.* **2010**, *1804*, 445-453.

16. Davis, M. I.; Hunt, J. P.; Herrgard, S.; Ciceri, P.; Wodicka, L. M.; Pallares, G.; Hocker, M.; Treiber, D. K.; Zarrinkar, P. P. Comprehensive analysis of kinase inhibitor selectivity. *Nat. Biotechnol*. **2011**, 29, 1046−1051.

17. Chang Y, Lu X, Shibu M A, et al. Structure Based Design of *N*-(3-((1 *H*-Pyrazolo [3, 4-*b*] pyridin-5-yl) ethynyl) benzenesulfonamides as Selective Leucine-Zipper and Sterile-α Motif Kinase (ZAK) Inhibitors. *J. Med. Chem*. **2017**, 60, 5927-5932.

18. Fabian, M. A.; Biggs, W. H., 3rd; Treiber, D. K.; Atteridge, C. E.; Azimioara, M. D.; Benedetti, M. G.; Carter, T. A.; Ciceri, P.; Edeen, P. T.; Floyd, M.; Ford, J. M.; Galvin, M.; Gerlach, J. L.; Grotzfeld, R. M.; Herrgard, S.; Insko, D. E.; Insko, M. A.; Lai, A. G.; Lelias, J. M.; Mehta, S. A.; Milanov, Z. V.; Velasco, A. M.; Wodicka, L. M.; Patel, H. K.; Zarrinkar, P. P.; Lockhart, D. J. A small molecule-kinase interaction map for clinical kinase inhibitors. *Nat. Biotechnol.* **2005**, *23*, 329-336.

19. Cheng, Y. C.; Kuo, W. W.; Wu, H. C.; Lai, T. Y.; Wu, C. H.; Hwang, J. M.; Wang, W. H.; Tsai, F. J.; Yang, J. J.; Huang, C. Y.; Chu, C. H. ZAK induces MMP-2 activity via JNK/p38 signals and reduces MMP-9 activity by increasing TIMP-1/2 expression in H9c2 cardiomyoblast cells. *Mol. Cell Biochem.* **2009**, *325*, 69-77.

20. Fu, C. Y.; Kuo, W. W.; Ho, T. J.; Wen, S.-Y.; Lin, L. C.; Tseng, Y. S.; Hung, H. C.; Viswanadha, V. P.; Yang, J. J.; Huang, C. Y. ZAKβ antagonizes and ameliorates the cardiac hypertrophic and apoptotic effects induced by ZAKα. *Cell Biochem. Funct*. **2016**, *34*, 606-612.

21. Hsieh, Y. L.; Tsai, Y. L.; Shibu, M. A.; Su, C. C.; Chung, L. C.; Pai, P. Y.; Kuo, C. H.; Yeh, Y. L.; Viswanadha, V. P.; Huang, C.Y. ZAK induces cardiomyocyte hypertrophy and brain natriuretic peptide expression via p38/JNK signaling and GATA4/c-Jun transcriptional factor activation. *Mol. Cell. Bio.* **2015**, *405*, 1-9.

22. Minor, W.; Cymborowski, M.; Otwinowski, Z.; Chruszcz, M. HKL-3000: the integration of data reduction and structure solution from diffraction images to an initial model in minutes. *Acta Cryst.* **2006**, *62*, 859-866.

Table of Contents graphic